

MODERN PATHOLOGY

 USCAP 2018

ABSTRACTS

PATHOBIOLOGY

(1934-1984)

107TH ANNUAL MEETING

GEARED



TO LEARN



MARCH 17-23, 2018

Vancouver Convention Centre
Vancouver, BC, Canada

Published by

SPRINGER NATURE

www.ModernPathology.org

 **USCAP**
Creating a Better Pathologist

AN OFFICIAL JOURNAL OF THE
UNITED STATES AND CANADIAN
ACADEMY OF PATHOLOGY

EDUCATION COMMITTEE

Jason L. Hornick, Chair
 Rhonda Yantiss, Chair, Abstract Review Board
 and Assignment Committee
 Laura W. Lamps, Chair, CME Subcommittee
 Steven D. Billings, Chair, Interactive Microscopy
 Shree G. Sharma, Chair, Informatics Subcommittee
 Raja R. Seethala, Short Course Coordinator
 Ilan Weinreb, Chair, Subcommittee for
 Unique Live Course Offerings
 David B. Kaminsky, Executive Vice President
 (Ex-Officio)
 Aleodor (Doru) Andea
 Zubair Baloch
 Olca Basturk
 Gregory R. Bean, Pathologist-in-Training
 Daniel J. Brat

Amy Chadburn
 Ashley M. Cimino-Mathews
 James R. Cook
 Carol F. Farver
 Meera R. Hameed
 Michelle S. Hirsch
 Anna Marie Mulligan
 Rish Pai
 Vinita Parkash
 Anil Parwani
 Deepa Patil
 Lakshmi Priya Kunju
 John D. Reith
 Raja R. Seethala
 Kwun Wah Wen, Pathologist-in-Training

ABSTRACT REVIEW BOARD

Narasimhan Agaram	Mamta Gupta	David Meredith	Souzan Sanati
Christina Arnold	Omar Habeeb	Dylan Miller	Sandro Santagata
Dan Berney	Marc Halushka	Roberto Miranda	Anjali Saqi
Ritu Bhalla	Krisztina Hanley	Elizabeth Morgan	Frank Schneider
Parul Bhargava	Douglas Hartman	Juan-Miguel Mosquera	Michael Seidman
Justin Bishop	Yael Heher	Atis Muehlenbachs	Shree Sharma
Jennifer Black	Walter Henricks	Raouf Nakhleh	Jeanne Shen
Thomas Brenn	John Higgins	Ericka Olgaard	Steven Shen
Fadi Brimo	Jason Hornick	Horatiu Olteanu	Jiaqi Shi
Natalia Buza	Mojgan Hosseini	Kay Park	Wun-Ju Shieh
Yingbei Chen	David Hwang	Rajiv Patel	Konstantin Shilo
Benjamin Chen	Michael Idowu	Yan Peng	Steven Smith
Rebecca Chernock	Peter Illei	David Pisapia	Lauren Smith
Andres Chiesa-Vottero	Kristin Jensen	Jenny Pogoriler	Aliyah Sohani
James Conner	Vickie Jo	Alexi Polydorides	Heather Stevenson-Lerner
Claudiu Cotta	Kirk Jones	Sonam Prakash	Khin Thway
Tim D'Alfonso	Chia-Sui Kao	Manju Prasad	Evi Vakiani
Leona Doyle	Ashraf Khan	Bobbi Pritt	Sonal Varma
Daniel Dye	Michael Kluk	Peter Pytel	Marina Vivero
Andrew Evans	Kristine Konopka	Charles Quick	Yihong Wang
Alton Farris	Gregor Krings	Joseph Rabban	Christopher Weber
Dennis Firchau	Asangi Kumarapeli	Raga Ramachandran	Olga Weinberg
Ann Folkins	Frank Kuo	Preetha Ramalingam	Astrid Weins
Karen Fritchie	Alvaro Laga	Priya Rao	Maria Westerhoff
Karuna Garg	Robin LeGallo	Vijaya Reddy	Sean Williamson
James Gill	Melinda Lerwill	Robyn Reed	Laura Wood
Anthony Gill	Rebecca Levy	Michelle Reid	Wei Xin
Ryan Gill	Zaibo Li	Natasha Rekhtman	Mina Xu
Tamara Giorgadze	Yen-Chun Liu	Michael Rivera	Rhonda Yantiss
Raul Gonzalez	Tamara Lotan	Mike Roh	Akihiko Yoshida
Anuradha Gopalan	Joe Maleszewski	Marianna Ruzinova	Xuefeng Zhang
Jennifer Gordetsky	Adrian Marino-Enriquez	Peter Sadow	Debra Zynger
Ilyssa Gordon	Jonathan Marotti	Safia Salaria	
Alejandro Gru	Jerri McLemore	Steven Salvatore	

To cite abstracts in this publication, please use the following format: **Author A, Author B, Author C, et al. Abstract title (abs#). *Modern Pathology* 2018; 31 (suppl 2): page#**

PATHOBIOLOGY

(INCLUDING PAN-GENOMIC/PAN-PROTEOMIC APPROACHES TO CANCER)

1934 The Landscape of Somatic Mutations in Advanced Breast Cancer: A Unique Population with Comparison to Public Studies

Sara E Abbott¹, Russell Broaddus², Hui Chen¹. ¹UT MD Anderson Cancer Center, Houston, TX, ²M.D. Anderson Cancer Center, Houston, TX

Background: The Cancer Genome Atlas (TCGA) and similar studies that followed have laid a strong foundation for characterizing primary breast cancers (BCs) at the genomic level. However, genomic heterogeneity may exist across different sites and time points of a disease course. Understanding how the genomic profile differs between advanced and early BCs will better delineate the pathobiology of more aggressive disease. We present the mutational profile of a unique population comprised exclusively of patients with treatment-resistant advanced BC presenting to a large tertiary care cancer center and compare our findings to both TCGA and the largest publically available dataset of metastatic BC (mBC).

Design: We included all advanced BC patients (n=83) who had 134-gene panel next generation sequencing (NGS) performed from 2016-2017. Metastatic/recurrent tumor was preferentially used for testing. Data for somatic mutation frequency in TCGA and the mBC study (Lefebvre, PLoS Med, 2016) were obtained via cBioportal.org. TCGA included predominantly primary breast tumors. The mBC study included all metastatic tumors, with a mix of treatment-naïve and treatment-resistant patients.

Results: The majority of tested tumors in our cohort were from recurrent and metastatic disease (80%), with a diverse range of distant metastatic sites represented (Table 1). A total of 6 genes were identified with somatic mutation frequencies significantly higher in our study population versus TCGA and/or the mBC study (Table 2). These included the 5 tumor suppressor genes *TP53* (59% vs 34% and 41%, respectively, p<0.001), *RB1* (8% vs 2% and 5%, p=0.001), *NOTCH1* (4% vs 1% and 1%, p=0.007), *TET2* (7% vs 1% and 1%, p<0.001), and *APC* (6% vs 1% and 2%, p=0.001), and the oncogene *ESR1* (14% vs 1% and 10%, p<0.001). The increase in *ESR1*, *TP53*, and *APC* appeared to occur preferentially in the ER+/HER2- group, while *RB1* and *NOTCH1* mutations were increased most in the triple negative (TNBC) group, and *TET2* mutations were increased in both.

Table 1. Location of tumor used for testing in advanced breast cancer patients in this cohort study

	Total Patients (n=83)	ER+/HER2- (n=40)	TNBC (n=30)	HER2+ (n=13)
Primary tumor	17 (20%)	3 (8%)	10 (33%)	4 (31%)
Local recurrence	9 (11%)	4 (10%)	4 (13%)	1 (8%)
Metastasis	57 (69%)	33 (83%)	16 (53%)	8 (62%)
Bone	3 (4%)	2 (5%)	0	1 (8%)
Brain	2 (2%)	1 (3%)	0	1 (8%)
Liver	25 (30%)	20 (50%)	3 (10%)	2 (15%)
Lymph node, distant	1 (1%)	1 (3%)	0	0
Lymph node, regional	5 (6%)	0	5 (17%)	0
Lung	12 (14%)	3 (8%)	5 (17%)	4 (31%)
Pelvic/peritoneal	5 (6%)	5 (13%)	0	0
Soft tissue	4 (5%)	1 (3%)	3 (10%)	0

Table 2. Comparison of common somatic mutation frequencies between this cohort and previous public studies

Number with mutation, n (%)	Tumor Suppressor Genes					Oncogene
	<i>TP53</i>	<i>RB1</i>	<i>NOTCH1</i>	<i>TET2</i>	<i>APC</i>	<i>ESR1</i>
Current study cohort (n=83)	49 (59%)	7 (8%)	3 (4%)	6 (7%)	5 (6%)	12 (14%)
ER+/HER2-, 40 (48%)	16 (40%)	1 (3%)	1 (3%)	3 (8%)	3 (8%)	9 (23%)
TNBC, 30 (36%)	27 (90%)	5 (17%)	2 (7%)	3 (10%)	1 (4%)	0
HER2+, 13 (16%)	6 (46%)	1 (8%)	0	1 (8%)	3 (23%)	0
TCGA (n=781)	269 (34%)	15 (2%)	4 (1%)	4 (1%)	7 (1%)	4 (1%)
ER+/HER2-, 512 (66%)	95 (19%)	4 (1%)	1 (0.2%)	3 (1%)	4 (1%)	4 (1%)
TNBC, 135 (17%)	114 (84%)	8 (6%)	2 (1%)	0	1 (1%)	0
HER2+, 134 (17%)	60 (45%)	3 (2%)	1 (1%)	1 (1%)	2 (1%)	0
Metastatic BC (n=205)	85 (41%)	10 (5%)	1 (1%)	2 (1%)	4 (2%)	20 (10%)
ER+/HER2-, 140 (68%)	38 (27%)	7 (5%)	0	2 (1%)	3 (2%)	20 (14%)
TNBC, 51 (25%)	38 (75%)	3 (6%)	1 (2%)	0	1 (2%)	0
HER2+, 14 (7%)	9 (7%)	0	0	0	0	0
P-value	<0.001	0.001	0.007	<0.001	0.001	<0.001

Conclusions: Our analysis of a unique population of patients with advanced BC identified increased mutation frequencies in 5 tumor suppressor genes (*TP53*, *RB1*, *NOTCH1*, *TET2*, *APC*) and an oncogene (*ESR1*). These findings are notable, as *TP53*, *RB1*, *APC* and *ESR1* are all proposed driver mutations in breast cancer. *TP53* and *ESR1* mutations have also been associated with worse prognosis in BC. *NOTCH1* and *TET2* mutations do not have a previously reported role in BC pathogenesis and may warrant further exploration.

1935 Loss of Nuclear FoxM1 Immunoreactivity Suggests Switch from Myc-FoxM1 to non-FoxM1 signaling in Double-Hit Lymphomas of Germinal Center Origin

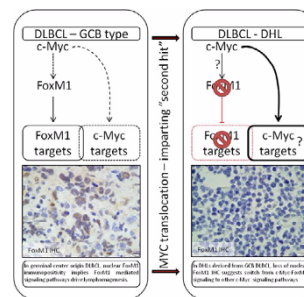
Aadil Ahmed¹, Austin McHenry², Kamran Mirza³. ¹Loyola University Medical Center, Maywood, IL, ²Loyola University Chicago Stritch School of Medicine, ³Loyola University Medical Center, Maywood, IL

Background: FoxM1 is a forkhead box transcription factor that

promotes cell cycle progression and prevention of growth arrest [Nat Rev Cancer 7(11):847-59]. Overexpression of FoxM1 is a driving feature of diffuse large B-cell lymphoma (DLBCL), with up to 84.6% of DLBCLs showing upregulation of this protein by immunohistochemistry (IHC) (Haematologica 2012 (97): 1092-1100). Double hit lymphoma (DHL) is an uncommon subtype DLBCL with rearrangements of two significant genes – the MYC gene and either the BCL2 or BCL6 genes (Genes 2017;8(4):8). Typically, FoxM1 is considered a downstream target of c-Myc signaling (Hepatology 2008; 48(4)1302-10). In this study, we evaluate the staining pattern of FoxM1 IHC in different groups of DLBCL and correlate with underlying c-Myc signaling and lymphoma biology.

Design: After appropriate IRB approval, archived formalin-fixed paraffin-embedded tissue with a diagnosis of DLBCL between 2013 and 2017 was retrieved from storage at our tertiary care academic medical center. Ten cases of DLBCL (germinal center origin), 5 cases of DHL (with FISH proven c-myc translocation) and 4 cases of DLBCL, non-germinal center origin were stained with FoxM1 antibody (Abcam 83097, 5ug/mL). Previous stains for CD10, BCL-2, BCL-6, Ki-67 and in some cases MUM1 were reviewed.

Results: All 10 cases of GCB origin DLBCL demonstrated focal, nuclear staining for FoxM1 (Figure 1). Most cases were positive for CD10 and all demonstrated high Ki-67 proliferation fractions. In contrast, all 5 cases of DHL demonstrated loss of nuclear FoxM1 staining (Figure 1) and had FISH evidence of MYC translocation.



Conclusions: This study represents only few cases; however, the consistency of this data suggest that while FoxM1 mediated signaling plays a role in the pathobiology of germinal center origin DLBCL; the addition of the 'second hit' by way of c-Myc translocation changes the signaling pathway to non-FoxM1 mediated lymphomagenesis. It is well known that FoxM1 is not the only c-Myc target gene and other possible targets include several cyclins, CDKs, and MCMs. These findings have a) diagnostic utility in that lack of FoxM1 staining implies DHL in cases of GCB DLBCL and b) further study of other c-Myc targets in DHL could isolate a predominant signaling pathway and facilitate new targeted therapeutic strategies.

1936 Key Cancer-Related Gene Mutations Are Rare Events In Goblet Cell Carcinoids Using A Next Generation Sequencing Approach

Andrew Bandy¹, Audrey Deeken-Draise², Ryan Jones³, Katrina Krogh⁴, Juehua Gao⁵, Maryam Pezhouh⁵, Guang-Yu Yang¹. ¹Chicago, IL, ²Northwestern Memorial Hosp, Chicago, IL, ³Naperville, IL, ⁴Northwestern Memorial Hospital, ⁵Northwestern University, Feinberg School of Medicine, Chicago, IL

Background: Goblet cell carcinoids (GCC) of the appendix are uncommon tumors with no well-defined pathogenesis. These tumors harbor mixed phenotypic features of both intestinal goblet cells as well as neuroendocrine cells. Pathologically it is not uncommon to identify malignant transformation from GCC to invasive adenocarcinoma, either mucinous/signet ring cell carcinoma or poorly differentiated adenocarcinoma; thus, GCC is managed clinically under colonic adenocarcinoma protocols from pathologic staging to adjuvant chemotherapy. However, there is little study on the genetic alterations that drive GCC carcinogenesis. Since GCC share common pathobiologic features with colonic adenocarcinoma, a panel of 22 key genes for their mutation profile was analyzed in a cohort of GCC specimens using a next generation sequencing (NGS) approach.

Design: Six cases of GCC were retrieved from our institution from 2010-2017. Histologic features, staging and follow up data of all cases were reviewed. Next generation sequencing was also performed on all tumors for analysis of hotspot mutations in key cancer related genes including KRAS, EGFR, BRAF, PIK3CA, AKT1, ERBB2, PTEN, NRAS, STK11, MAP2K1, ALK, DDR2, CTNBN1, MET, TP53, SMAD4, FBX7, FGFR3, NOTCH1, ERBB4, FGFR1/2.

Results: All six patients presented clinically with acute appendicitis with a median age of 59 (range 44-79 years). Five (5/6, 83%) cases were pT3 (two of which demonstrated positive surgical margin) and one case was pT4 with widespread metastases into the peritoneum. Two cases (2/6, 33%) showed transformation from GCC into signet ring cell carcinoma, while the remaining four cases (4/6, 67%) showed

traditional GCC. Hotspot mutations in these twenty-two colon cancer-related genes were not detected in these six cases of GCC using an NGS approach.

Conclusions: Our study demonstrates that key cancer-driving gene mutations are extremely rare, if at all present, in GCC of the appendix, among the genes included in our 22-gene panel. This indicates that alternative pathways exist in the pathogenesis of GCC, particularly compared to colonic adenocarcinomas, and that separate treatment options may need to be considered. All cases of GCC in this cohort were advanced pathologic stage (\geq pT3), and three (3/6, 50%) demonstrated positive margins or distant spread indicative of the need for further clinical management.

1937 Thyroid Nodule Size Correlates with Bethesda Diagnostic Categories, Genetic Mutation and miRNA Classifier Status: Pathobiologic Implications

Anna B Banizs¹, Sarah Jackson², Christina Narick³, Jan F Silverman⁴, Sydney Finkelstein². ¹Allegheny General Hospital, Pittsburgh, PA, ²Interpace Diagnostics, ³Interpace Diagnostics, Pittsburgh, PA, ⁴Allegheny General Hospital, Allegheny Health Network, Pittsburgh, PA

Background: Size and pattern assessed by imaging modalities are critical parameters in the initial evaluation of thyroid nodules. Correlation of nodule size to cytology, mutational status and RNA classifier status provide valuable information toward cancer risk assessment. We used a large database (n=4295) to compare size of thyroid nodules across 1.) Bethesda Diagnostic Categories (BDC I-VI); 2.) groups with single mutation (*BRAF*, *RAS*, *PAX8/PPAR*), and 3.) risk-categories based on expression of microRNA (miRNA) classifier status.

Design: Cytology diagnosis was based on submitted cytology reports sorted into BDC I-VI and included size of thyroid nodules. Mutational analysis containing common mutations (*BRAF*, *RAS*, and *PAX8/PPAR*) was performed on next generation sequencing (Illumina). Classifier utilized a 10 miRNA panel trained on 257 thyroid reactive, benign, malignant specimens. For statistical comparison Mann-Whitney Rank Sum Test was used.

Results: Sizes of thyroid nodules in BDC-V and BDC-VI were significantly smaller, 1.95 and 1.92 cm compared to sizes in BDC-II, III and IV (P<0.001) 2.69, 2.41 and 2.55 cm, respectively. No significant difference between BDC-V and BDC-VI was found. Also, BDC-II, III and IV showed no significant size differences.

When groups with single mutation were compared; nodules with *PAX8/PPAR* mutation showed significantly greater size, 4.13 cm (P<0.001) to all other groups. Nodule size with *BRAFV600E* mutation, 1.73 cm, was significantly lower than nodules with *HRAS* 2.62 cm, *KRAS*, 2.28 cm and *NRAS* 2.61 cm (P<0.001). Groups with *HRAS*, *KRAS*, *NRAS* or *BRAFx* mutations showed no statistical differences.

When miRNA risk-categories were compared, the high risk/malignant category demonstrated a significantly smaller size compared to all other categories (P<0.001). No statistical difference was found between lower risk categories. High risk/malignant category held a significantly smaller size compared to all other categories when *BRAFV600E* mutated cases were removed. <

Conclusions: Based on a large database malignant/more aggressive status –assessed by cytology, mutational analysis or miRNA classifiers– was associated with a smaller nodule size. Nodules with *BRAFV600E* tended to be the smallest. High risk/malignant category without *BRAFV600E* mutation still represented a significantly smaller nodule size compared to other classifier groups. These molecular pathologic findings suggest that commitment to malignancy can occur very early in small size nodules.

1938 AKR1C1 Controls Cisplatin-resistance in Head and Neck Squamous Carcinoma Cells and is a Poor Prognosis Predictor

Wei-Min Chang¹, Michael Hsiao². ¹Academia Sinica, Taipei, Taiwan, ²Academia Sinica

Background: Cisplatin is the first line chemotherapy medication used to treat solid cancers. In head and neck squamous carcinoma (HNSCC), the sensitivity to cisplatin remains the key issue in successful cancer treatment. Genetic heterogeneity and aberrant protein expression may be the intrinsic factors that cause cisplatin resistance. Combination of the HNSCC gene expression data from Cancer Cell Line Encyclopedia (CCLE) and cisplatin sensitivity results (IC_{50}) from Genomics of Drug Sensitivity in Cancer (GDSC) revealed that Aldo-Keto Reductase Family 1 Member C1 (AKR1C1) may be associated with cisplatin sensitivity in HNSCC cells.

Design: We examined the expression levels of AKR1C1 and its correlated cisplatin IC_{50} in HNSCC cell lines. We then validated the *in vitro* and *in vivo* AKR1C1 functions in cisplatin sensitivity through complementary over-expression and knockdown assays, respectively.

We also used the domain-negative AKR1C1 and enzymatic inhibitor to examine the cisplatin resistance response of AKR1C1. Finally, we used the cDNA microarrays to identify the up-stream regulator that can modulate AKR1C1 overexpression in HNSCC cells to elucidate its molecular mechanism.

Results: We found that AKR1C1 expression positively correlate to HNSCC cisplatin sensitivity in HNSCC cells. AKR1C1 also acts as poor prognostic and recurrence markers in HNSCC patient cohort. Silencing of AKR1C1 expression not only reduced the *in vitro* cisplatin IC_{50} but also significantly suppressed FaDu and HSC-2 *in vivo* tumorigenicity after cisplatin treatment. Enforced AKR1C1 overexpression enhanced Cal-27 cell cisplatin resistance and increased *in vivo* tumorigenicity after cisplatin treatment. The enzymatic function of AKR1C1 and AKR1C1 microarray data analyses revealed the putative mechanistic role of AKR1C1 in inducing cisplatin resistance in HNSCC cells.

Conclusions: AKR1C1 is a crucial regulator for cisplatin resistance induction in HNSCC cells and is a poor prognostic marker for HNSCC patients. Targeting AKR1C1 may provide a new therapeutic strategy to treat HNSCC patients refractory to cisplatin treatment.

1939 PREVIOUSLY PUBLISHED

1940 Unique Mutant Gene Profile in a Cohort of IBD-Associated Flat Dysplasia Using Next Generation Sequencing Approach

Audrey Deeken-Draisey¹, Andrew Bandy², Ryan Jones³, Jie Liao⁴, Leyu Sun⁵, Katrina Krogh⁶, Maryam Kherad Pezhouh⁷, M. Sambasiva Rao⁸, Juehua Gao¹, Guang-Yu Yang². ¹Northwestern Memorial Hosp, Chicago, IL, ²Chicago, IL, ³Naperville, IL, ⁴Northwestern University, Chicago, IL, ⁵Northwestern, Chicago, IL, ⁶Northwestern Memorial Hospital, ⁷Northwestern University, Feinberg School of Medicine, Chicago, IL, ⁸Northwestern University, Chicago, IL

Background: Carcinogenesis of IBD is presumed to be due to increased chronic inflammation causing genetic alteration, and often is detected early by the diagnosis of dysplastic change with *TP53* missense mutation often identified. However, whether other key cancer-related genetic alterations in collaboration with mutant *TP53* gene lead to carcinogenesis is not well studied. Mutational analysis by Next Generation Sequencing (NGS) is a useful tool to identify mutations within dysplasia and carcinoma. Utilizing NGS with IHC, we aim to analyze the mutation profile of cancer related genes and expression of mutant *TP53* to characterize the key genetic alteration in IBD-associated flat dysplasia using a single institution large cohort.

Design: Searching the past 5 years at our institution, 15 patients with IBD-associated flat dysplasia were identified and 5 IBD-associated colonic adenocarcinomas were selected as control. 22 key cancer-related gene profiles were analyzed using NGS: *AKT1*, *ALK*, *BRAF*, *CTNNB1*, *DDR2*, *EGFR*, *ERBB2*, *ERBB4*, *FBXW7*, *FGFR1*, *FGFR2*, *FGFR3*, *KRAS*, *MAP2K1*, *MET*, *NOTCH1*, *NRAS*, *PIK3CA*, *PTEN*, *SMAD4*, *STK11*, and *TP53*. IHC for P53 or Ki-67 was performed on selected slides from each specimen with appropriate controls. Nuclear positivity of P53 or Ki-67 in epithelial cells or lesional area from 5 high power fields was analyzed. P53 positive staining was calculated as positive staining cells <, =, or > Ki-67 labeled proliferative cells.

Results: 87% (13/15) dysplasia had missense *TP53* mutation. All occurred in DNA-binding domain at exon 4 to 8 and no specific hot-spot mutation was seen. 47% (7/15) dysplasia carried other genetic alterations including 5 *KRAS* mutation, one *NOTCH1*, one *DDR1*, one *STK11* and one *FGFR3* (in which two cases had both *KRAS* and *NOTCH1* or *DDR1* mutation). Adenocarcinomas showed similar results as dysplasia that 3/5 cases carried missense *TP53* mutation and 2/5 had either *KRAS* or *BRAF* mutation. Immunostaining results showed all missense *TP53* mutant dysplasia or adenocarcinoma displayed mutant P53 protein accumulation with intense P53 nuclear staining and the ratio of P53/Ki-67 positive cells were > or =1 in IBD-dysplasia.

Conclusions: Within IBD-associated dysplasia: 1) missense *TP53* mutation is the most common/dominant genetic alteration, and 2) *TP53* combined with other gene mutation, particularly the *KRAS* oncogene appears crucial leading to carcinogenesis. Detection of these mutant genes with either NGS or IHC are practical for early detection of precancerous lesion – dysplasia.

1941 SOX11: A Multipotential Marker in Surgical Pathology A Systematic Analysis of SOX11 Expression in Epithelial and Nonepithelial Tumors

Yaqi Duan¹, San Peng Xu², Yuting Dong³, Guoping Wang³. ¹Institute of Pathology, Tongji Hospital, Tongji Medical College of Huazhong University of Science and Technology, Wuhan, ²Wuhan, Hubei ³Institute of Pathology, Tongji Hospital, Tongji Medical College of Huazhong University of Science and Technology, Wuhan, Hubei

Background: SOX11 is an essential transcription factor for neurogenesis. Recently SOX11 has been found to be overexpressed in

mantle cell lymphoma, thus is a valuable diagnostic marker. However the diagnostic utility of SOX11 has never been comprehensively studied.

Design: Here formalin-fixed, paraffin-embedded tissue samples for 1722 primary neoplasms and the paired peritumoral tissues were subjected to SOX11 immunostain.

Results: We found that SOX11 was not identified in any peritumoral parenchymal or mesenchymal tissues and benign tumors and borderline tumors except for weak and focal staining in 1 (6%) salivary pleomorphic adenoma. In malignant tumors, consistent with its involvement in neurogenesis prominent nuclear staining of SOX11 was observed in all neuroectodermal tumors with variable neural differentiation such as 38 PNET/EWSs, 28 medulloblastomas, 8 esthesioneuroblastomas, 11 neuroblastomas and 11 central neurocytomas, and while less frequent and weak expression was found in tumors with glial differentiation including 5 (24%) malignant peripheral nerve sheath tumors and 7 (50%) astrocytomas. Besides strong expression was also identified in area of all 12 immature teratomas demonstrating embryonic neural differentiation. Among malignant epithelial tumors neuroendocrine tumors have certain neuronal features. Interestingly SOX11 was identified in some of including 85 (60%) pulmonary high-grade neuroendocrine carcinomas (NECs), and 7 (16%) extrapulmonary high-grade NECs. In contrast, only 1 (2%) low-grade NE tumor showed weak and focal expression. In addition to NECs, expression of SOX11 was identified in 36 (97%) salivary ductal carcinomas and less frequently 6 (17%) breast carcinomas. Besides there were scattered staining for 3 (15%) ovarian serous carcinomas and weak focal staining for 1 (2%) pulmonary adenocarcinoma, 2 (18%) epithelial-myoepithelial carcinomas and 3 (25%) yolk sac tumors. In malignant mesenchymal tumors distinct SOX11 expression was identified in 32 (97%) rhabdomyosarcomas, 14 (100%) myxoid liposarcomas, 15 (83%) MCLs and less frequently 2 (9%) T/B lymphoblastic lymphomas. Weak focal staining was noted in 11 (36%) synovial sarcoma, 3 (10%) angiosarcoma and 2 (20%) Burkitt lymphomas. SOX11 was not seen in other neoplasms.

Table 1. SOX11 expression in neuroectodermal tumors

Tumor type	Positive/Total, n (%)
PNET/Ewing	38/38(100%)
Medulloblastoma	28/28(100%)
Neuroblastoma	11/11(100%)
Esthesioneuroblastoma	8/8(100%)
Central neurocytoma	11/11(100%)
Astrocytoma (I-IV)	7/14(50%)
Malignant peripheral nerve sheath tumor	5/21(24%)

Table 2. SOX11 expression in epithelial tumors

Tumor type	Positive/Total, n (%)
Lung	
Squamous carcinoma	0/62(0%)
Adenocarcinoma	1/52(2%)
Large cell carcinoma	2/57(4%)
Carcinoid	0/25(0%)
Atypical carcinoid	1/12(8%)
Small cell carcinoma	69/100(69%)
Large cell neuroendocrine carcinoma	16/41(39%)
Digestive system	
Squamous carcinoma (esophagus)	0/11(0%)
Adenocarcinoma (stomach, colon, bile duct, pancreas)	0/28(0%)
Hepatocellular carcinoma	0/12(0%)
NET (G1)	0/16(0%)
NET (G2)	0/8(0%)
Extrapulmonary	
Small cell carcinoma	7/45(16%)
Large cell neuroendocrine carcinoma	
Female genital tract	
Adenocarcinoma (cervix, uterus, ovary)	3/50(6%)
Squamous carcinoma (cervix)	0/11(0%)
Sexual-stromal tumor	0/16(0%)
Germ cell tumors,	5/23(22%)
Embryonic carcinoma	0/9(0%)
Yolk sac tumor	3/12(25%)
Seminoma/dysgerminoma	0/12(0%)
Choriocarcinoma	0/11(0%)
Mature teratoma	0/6(0%)
Immature teratoma	12/12(100%)
Breast	
Breast carcinoma	6/36(17%)
Kidney	
Renal cell carcinoma	0/11(0%)
Urothelial carcinoma	0/15(0%)
Prostate	
Adenocarcinoma	0/7(0%)
Salivary gland	
Pleomorphic adenoma	0/17(6%)
Acinar cell carcinoma	0/18(0%)
Salivary duct carcinoma	34/35(97%)
Adenoid cystic carcinoma	0/21(0%)
Mucoepidermoid carcinoma	0/25(0%)
Epithelial-myoepithelial carcinoma	2/11(18%)
Myoepithelial carcinoma	0/3(0%)
Secretory carcinoma	0/11(0%)
Nasopharyngeal	
Nasopharyngeal carcinoma	0/11(0%)
Adrenal	
Cortical adenoma/carcinoma	0/6(0%)
Thymus	
Thymoma/thymic carcinoma	0/20(0%)
Thyroid	
Thyroid papillary carcinoma	0/17(0%)
Thyroid medullary carcinoma	0/16(0%)
Parathyroid	
Parathyroid carcinoma	0/8(0%)
Skin/mouth	
Squamous carcinoma	0/10(0%)

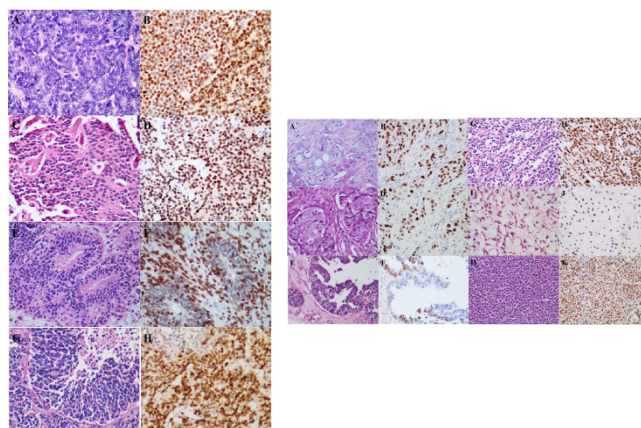


Table 3. SOX11 expression in mesenchymal tumors

Tumor type	Positive/Total, n (%)
Lymphatics	
Mantle cell lymphoma	15/18(83%)
Follicular lymphoma	0/42(0%)
Burkitt lymphoma	2/10(20%)
Large B cell lymphoma	0/110(0%)
T/B cell lymphoblastoma	2/22(9%)
MALT*	0/28(0%)
Angioimmunoblastic Tcell lymphoma	0/3(0%)
NK/T cell lymphoma	0/3(0%)
Small lymphocytic lymphoma	0/4(0%)
Peripheral T cell lymphoma	0/5(0%)
Angiosarcoma	3/30(10%)
Leiomasarcoma	0/7(0)
Liposarcoma	9/36(25%)
Rhabdoid sarcoma	32/33(97%)
Malignant melanoma	0/8(0%)
Dermatofibrosarcoma protuberans	0/5(0%)
Solitary fibrous tumor	0/11(0%)
Fibrosarcoma	0/5(0%)
Undifferentiated sarcoma	0/10(0%)
Synovial sarcoma	10/28(36%)
Alveolar soft part sarcoma	0/7(0%)
Epithelioid sarcoma	0/17(0%)
Gastrointestinal stromal tumor	0/10(0%)
Chondrosarcoma	0/5(0%)
Osteosarcoma	1/8(12%)

*MALT: mucosa-associated lymphoid tissue lymphoma

Conclusions: Therefore, SOX11 is a sensitive and specific marker for malignant neuroectodermal tumors, immature teratoma, high grade-NECs, salivary duct carcinoma, breast carcinoma, rhabdomyosarcoma, MCL and myxoid liposarcoma.

1942 Biallelic EGFR Amplification as a Pattern-Based Biomarker in EGFR-Driven Cancers

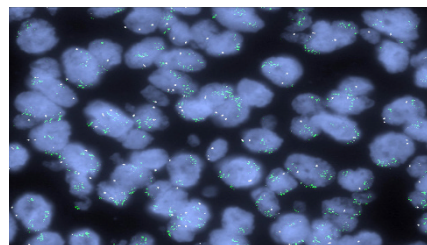
Adam Fisch¹, Ibiayi Dagogo-Jack², Ryan P Frazier¹, Carissa Desilus¹, Jochen Lennerz³, John Iafrate¹. ¹Massachusetts General Hospital, Boston, MA, ²Massachusetts General Hospital, ³Massachusetts General Hospital and Harvard Medical, Boston, MA

Background: Epidermal growth factor receptor (EGFR) amplification is an acknowledged and well-characterized oncogenic event in several cancers. While assessment of gene amplification at the cellular level is routinely available and gene-to-copy number (GCN) cutoffs have been established using fluorescent in situ hybridization (FISH), biallelic EGFR amplification patterns have not been widely examined.

Design: We re-examined a case series of all FISH assays testing positive for EGFR amplification from September 2016 to September 2017. We included the primary tumor site, the number of EGFR and CEP7 signals, the GCN-ratio, and at least 2 representative images of tumor nuclei. We assessed nuclei with at least diploid (≥ 2) CEP7 signals. Based on the distribution pattern of EGFR signals (green in Figure 1) to CEP7 signals (white in Figure 1) we distinguished three patterns: only "monoallelic" amplification with EGFR signals clustered in proximity to a distinct CEP7; presence of "biallelic" amplification as two distinct groups of EGFR clustered around respective CEP7 signals; "indistinct" encompasses diffuse EGFR amplification, amplification too numerous to count (GCN > 25), amplification with underlying polysomy, and cases where CEP7 signals were too close to distinguish nuclear territories.

Results: A total of 51 EGFR-amplified cases (n = 30 CNS, 17 lung, 4 gastrointestinal) were reviewed, and an overview of the amplification pattern is shown in Table 1. Notably, two cases of biallelic EGFR amplification occurred in EGFR-mutant lung cancer patients at time of progression on tyrosine kinase inhibitor (TKI) therapy (re-biopsy specimen). Review of the original samples showed no amplification and next-generation sequencing data showed, when corrected for cellularity, a ~1:1 estimated ratio of mutant to wild-type alleles. These findings indicate that wild-type and mutation-specific amplification of EGFR may contribute to TKI adaptations.

Tissue	Total #	# of Monoallelic (%)	Pattern	
			# of Biallelic (%)	# of Indistinct (%)
CNS	30	2 (6%)	12 (40%)	12 (40%)
Lung tumor	17	6 (35%)	6 (35%)	5 (30%)
Gastrointestinal	4	N/A	2 (50%)	2 (50%)
All	51	8 (16%)	20 (39%)	19 (37%)



Conclusions: With biallelic EGFR amplification observed in 39% of our series, it is more common than anticipated. The pattern is generally not captured when reporting GCN ratios. Our data provide a starting point to explore the clinical relevance of biallelic EGFR amplification as a biomarker – and in particularly the relevance in the setting of TKI resistance.

1943 Next Generation Sequencing Identifies Mutational Differences Between Primary and Metastatic Colorectal Carcinoma: Therapeutic Implications for Specimen Selection

Joseph S Frye¹, Eric Vaiñ², Sarah Imam³, Andy Pao², Angela Aguiluz², Wenjuan Zhang², Jianbo Song², David Engman⁴, Brent K Larson⁵, Deepti Dhal⁶, Maha Guindi⁷, Jean Lopategui⁸. ¹Cedars Sinai Medical Center, Los Angeles, CA, ²Cedars-Sinai Medical Center, ³Cedars Sinai Medical Center, ⁴Los Angeles, CA, ⁵Cedars-Sinai Medical Center, West Hollywood, CA, ⁶Cedars-Sinai Medical Center, Los Angeles, CA, ⁷Cedars-Sinai Med Ctr, Beverly Hills, CA, ⁸West Hollywood, CA

Background: Colorectal carcinoma (CRC) is a common and aggressive malignancy for which standard chemotherapy is of limited benefit in the metastatic setting. While a few studies have suggested that KRAS, NRAS, and BRAF mutations are highly concordant in paired primary and metastatic CRC, others have shown considerable heterogeneity. It has not been previously elucidated whether this is due to tumor heterogeneity or clonal evolution. We aim to explore the mutational landscape in paired primary and metastatic colorectal tumors.

Design: Paired primary and metastatic CRC from 14 patients were sequenced using NGS. Of those, 5 with discordant results were selected for further sequencing. Their primary tumor and metastasis were multiply sampled to obtain 21 formalin-fixed paraffin-embedded samples. The discordant samples included 5 primary tumors, 1 regional lymph node metastasis and 5 distant organ metastases. Samples were sequenced with the 50-gene AmpliSeq cancer panel v2 on an Ion Torrent PGM sequencing instrument (Thermo Fisher, Inc.), targeting 2855 hotspot mutations.

Results: All five patients showed heterogeneity in the primary or metastatic sites. One patient had completely discordant results with a TP53 frameshift deletion in the primary and TP53 deletion and APC point mutations in the metastasis. Clinically relevant mutations in genes including APC, ATM, NRAS, PIK3CA and TP53 were either gained (n=11) or lost (n=5) in distant metastases. Across all patients, 48 clinically relevant mutations were identified involving 12 genes: TP53, APC, KRAS, NRAS, PIK3CA, FLT3, FGFR3, STK11, CTNBN1, JAK3, KDR and CDKN2A. Thirty four mutations (71 %) were concordant between primary tumors and distant metastases.

Conclusions: Evidence from our study shows mutational discordance in paired primary and metastatic tumors. Our data suggests that while some mutations are present in both the primary and metastasis there is significant mutational tumor heterogeneity amongst the samples in the primary and metastatic sites. Metastatic samples lost or gained additional mutations compared to the primary tumor indicative of clonal evolution. This suggests that treatment selection should ideally be based on sequencing information from multiple samples of the same tumor and that genetic profiling should be performed on the most recent tissue samples, including metastases.

1944 NUTM1 Gene Rearranged Neoplasia

Zoran Gatalica¹, Jeffrey Swensen², Todd M Stevens³, Margaret Brandwein-Weber⁴, Joanne Xiu², Markku Miettinen⁵, Julia Bridge⁶. ¹Caris Life Sciences, Phoenix, AZ, ²Caris Life Sciences, ³University of Alabama at Birmingham, Birmingham, AL, ⁴Mt. Sinai Hospital, New York, NY, ⁵National Cancer Institute, ⁶Nebraska Medicine, Omaha, NE

Disclosures:

Zoran Gatalica: *Employee*, Caris Life Sciences
Jeffrey Swensen: *Employee*, Caris Life Sciences
Joanne Xiu: *Employee*, Caris Life Sciences

Background: NUT midline carcinoma (NMC) is a rare, genetically defined, aggressive malignancy defined by rearrangements of the NUTM1 gene most commonly fused to BRD4 or BRD3 genes. Typical histologic features associated with NMC are those of an

epithelial malignancy with “abrupt” squamous differentiation. We have systematically evaluated different histologic types of solid malignancies for NUTM1 gene rearrangements.

Design: Fusion genes and variant transcripts were systematically analyzed in over 10100 solid malignancies (Caris Life Sciences, Phoenix, AZ) utilizing Archer FusionPlex Solid Tumor panel, (ArcherDX, Inc. Boulder, CO). Secondary confirmation of the fusion gene was achieved using specific RT-PCR amplification and Sanger sequencing. Additional cases of NMC were retrieved from the Nebraska Medical Center and the University of Alabama at Birmingham. NUTM1 gene rearrangements (break-apart and fusion probes) and NUT protein expression were evaluated in select cases using standard FISH and IHC, respectively.

Results: NUTM1 gene rearrangements were identified in 21 patients including one with both primary and metastatic tumor analyzed. Patients presented with primary lung (x7), base of skull/sinus (x7), soft tissue/bone (x2), glottis, ovary, lacrimal sac, liver and mediastinal malignancies. NUTM1 fusion partners included: BRD4 (x16), NSD3 (x2), BRD3 and MGA. The fusion partner for one case was not defined. All fusion types were independently confirmed (FISH and/or RT-PCR). IHC showed expression of NUT protein in 2/2 cases (BRD4-NUTM1 and a novel MGA-NUTM1 fusion case of metastatic spindle cell neoplasm). Histologically, 11 cases were considered poorly differentiated lung carcinomas, 7 squamous cell carcinomas, 2 spindle cell malignancies (one in the lung, the other in soft tissue) and one large cell neuroendocrine carcinoma. A single patient with paired primary (lung) and metastatic (liver) tumor showed an identical NUTM1-NSD3 fusion in both sites.

Conclusions: Diagnosis of NMC is genetically defined by NUTM1 rearrangement. NMC presenting at an unusual site or lacking characteristic histopathologic features poses a significant challenge for diagnosis. It is important to detect and define NUTM1 gene fusion in all suspect cases due to the effective, targeted therapy of NMC with bromodomain and extra-terminal (BET) inhibitors. However, some novel NUTM1 fusions (e.g. MGA:NUTM1 detected in this series) may not be susceptible to the BET inhibition, and additional functional studies are needed.

1945 Hormonal, Stem Cell and Autoimmune Inflammatory Signaling as Possible Mechanisms of Disease in Hidradenitis Suppurativa: a Systems-Level Transcriptomic Analysis

Timothy D Gauntner, Chicago, IL

Background: Hidradenitis Suppurativa (HS) is a chronic inflammatory skin disease affecting the intertriginous axillary and groin skin. Although the inflammatory nature of HS is well-described, its pathobiology remains poorly understood. A hormonal basis for the disease has been suggested due to multiple risk factors relating to states of hormonal dysregulation, as well the fact that the disease is thought to arise from the pilosebaceous unit (PSU), which is regulated by androgens. Since the bulge of the PSU is also the location of epidermal stem cells, the pathogenesis of HS may also involve alterations in stem cell activity. Deciphering the molecular pathogenesis of HS will facilitate development of definitive therapeutics and prevention strategies for this debilitating disease.

Design: This work is an analysis of publicly available, human gene expression microarray data derived from skin biopsies taken from 17 patients with HS, including 13 patient-matched control biopsies. Gene expression profiles of HS skin were compared to those of control skin to identify key differentially-regulated biological pathways that may provide insight into disease pathogenesis. Multiple bioinformatic approaches focusing on transcriptional, positional, gene-ontological and pathway-enrichment readouts were utilized to construct a hypothetical model of the molecular pathogenesis of HS.

Results: Results demonstrate increased expression of genes under transcriptional control of androgen receptor in HS. Genes under control of the stem cell transcription factors Nanog and TP63 are also upregulated in HS. Analysis of the chromosomal position of genes upregulated in HS shows enrichment of 22 genes that reside on chromosomal cytoband 1q21-1q25, a known causative genetic locus in familial HS linked to Notch signaling. Functional pathway analysis of these 22 genes shows enrichment for keratinocyte differentiation and epidermis development pathways. Gene set enrichment analysis of the global transcriptomes of HS lesion and non-lesion skin demonstrates upregulation of the allograft rejection pathway.

Conclusions: These results are consistent with a disease model involving hormonal dysregulation of stem cell differentiation dynamics in the setting of autoimmune inflammation. This model unifies known epidemiological risk factors and key emerging concepts regarding the molecular pathogenesis of HS. The model also includes multiple pathways targetable with existing therapeutics, highlighting the clinical relevance of these findings.

1946 Tumor Molecular Profile as a Complement to Conventional Histology in the Diagnosis of Anaplastic Thyroid Carcinoma

Kanika Goel¹, Jan F Silverman², Christina Narick³, Sydney Finkelstein⁴. ¹Allegheny General Hospital, Pittsburgh, PA, ²Allegheny General Hospital, Allegheny Health Network, Pittsburgh, PA, ³Interpace Diagnostics, Pittsburgh, PA, ⁴Interpace Diagnostics

Background: Anaplastic thyroid carcinoma (ATC) represents the most advanced state of neoplastic progression in thyroid contrasting with most thyroid tumors that are well or partially differentiated. While the prognosis for the majority of thyroid cancers is very good, ATC represents a subset with predictable poor outcome. The molecular basis for anaplastic transformation in thyroid is not well understood. We sought to evaluate the role of tumor suppressor gene loss as a contributor to thyroid anaplasia.

Design: Unstained FFPE slides from ten specimens (primary and metastases) obtained from six ATC patients were micro-dissected and analyzed retrospectively for (i) oncogene point mutations (including *BRAF*, *RAS*, *PIK3CA*, *PAX8/PPAR*, *RET/PTC* translocations) using next generation sequencing; (ii) tumor suppressor gene (*TSG*) deletion as detected by loss of heterozygosity analysis using a panel of 24 markers linked to 10 TSGs (1p, 3p, 5q, 9p, 10q, 17p, 17q, 19q, 21q, 22q); (iii) *TERT* promoter point mutational analysis affecting base 124 (C to T).

Results: Oncogene point mutations (*BRAF V600E*) were detected in 4/6 ATC (66.7%). *TERT* promoter mutation (C124T) was detected in 2/6 ATC (33.3%). *TSG* deletion was detected in all ATC ranging from 2-8 affected loci. Common genomic loci showing LOH included 3p, 9p, 17p and 18q. No significant difference was observed between the molecular profile of primary and metastatic disease.

Conclusions: While *BRAF V600E* point mutation was frequently detected in ATC, this acquired mutation is typically found in better differentiated forms of thyroid cancer. *TERT* point mutation, a known predictor of aggressive thyroid tumor biology, was present in a minority of ATC. We show that *TSG* deletion appears to be universally associated with ATC and that may play a critical role in anaplastic transformation. It can help establish a definitive diagnosis and potentially provide information for targeted therapy.

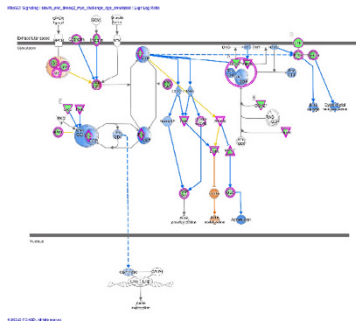
1947 Rho GDP-Dissociation Inhibitor Signaling is Upregulated in Myofibroblasts in Asthmatic Airways After Allergen Challenge

Paul Gordon¹, Tarah Lynch¹, Elaine De Heuvel¹, Carol Gwozd¹, Margaret Kelly². ¹University of Calgary, ²Foothills Medical Center, Calgary, AB

Background: Asthma is characterized by airway inflammation and episodic bronchoconstriction, secondary to an underlying dysfunction of the airway, termed airway hyperresponsiveness, AHR, believed to be related to structural changes, ‘airway remodeling’. Myofibroblasts rapidly increase in the airway submucosa after allergen challenge, in parallel with increased AHR and are believed to play a pivotal role in airway remodeling. However the pathobiology of the myofibroblast is poorly understood. Our aim was to characterize highly expressed genes in myofibroblasts in order to identify therapeutic targets against airway remodeling.

Design: Endobronchial biopsies were obtained from 12 mild asthmatic subjects 24 h after sham bronchial challenge and allergen challenge. Biopsies were snap-frozen, myofibroblasts and smooth muscle cells microdissected and RNA extracted. RNA from each cell type and challenge were pooled for Next Generation Sequencing, Illumina NextSeq 500 platform. Linear models of experimental factors compared myofibroblast-specific challenge differential expression relative to sham treated smooth muscle. The resultant data were analysed by two bioinformatics pipelines for transcript mapping, quantification and differential expression analysis, namely BWA with DESeq2 (generalized linear model at the gene level) and Kallisto with Sleuth (general linear model at the transcript level with 100 bootstraps). Concordant results from both pipelines were further investigated using Ingenuity Pathway Analysis software (Qiagen) to characterize the overarching pathways involved.

Results: 57 of the 173 genes involved in Rho GDP-Dissociation Inhibitor (RhoGDI) signaling are differentially regulated in myofibroblasts after allergen challenge, (Fischer’s Exact Test p-value 1.7e-5), with FDR corrected Wald p-value < 0.05 in both analysis pipelines. Fig. 1 shows the canonical pathway for RhoGDI signaling and molecules that are upregulated (red) or downregulated (green) by allergen challenge, including downstream predicted inhibition of actin stabilization (orange) and activation of cytoskeleton reorganization (blue).



Conclusions: RhoGDI controls Rho family GTPases which play an important role in multiple cell functions, including morphology, migration and gene transcription. By examining the regulation of this pathway in activated myofibroblasts, we hope to attain a great understanding of the genesis and function of these cells, and identify therapeutic targets to ameliorate airway remodeling.

1948 Off-Label Use of PD-L1 (22C3) Reveals Expression Trends: A Reference Laboratory Experience

Cassi B Grotepas¹, Jordan Abawi², Joshua F Coleman², Larissa Furtado¹, Allie Grossmann¹, Anna P Matynia¹, Amy Sandoval², Deepika Sirohi², Georgios Deftereos¹. ¹University of Utah, Salt Lake City, UT, ²ARUP Laboratories, ³University of Utah, Salt Lake City, UT

Background: Immune checkpoint inhibitor treatment is one of the most promising areas in solid tumor oncology. The PD-L1 22C3 pharmDx immunohistochemistry (IHC) test is approved by the US Food and Drug Administration (FDA) as a companion diagnostic in first and second line treatment with pembrolizumab (Keytruda®, Merck) for patients with non-small cell lung cancer (NSCLC). Pembrolizumab is FDA approved for other solid tumors, including head and neck squamous cell carcinoma (HNSCC), melanoma, urothelial carcinoma, and mismatch repair protein deficient/microsatellite unstable malignancies. However, for these tumors and other malignancies, 22C3 IHC is ordered outside of FDA indications, as an off-label test. In recent months, our IHC laboratory has received hundreds of off-label testing requests for 22C3 IHC. The purpose of this study was to quantify this volume, determine types of tumors being tested in this setting and identify possible correlations between 22C3 expression and clinicopathological variables.

Design: Our institutional database was queried for all PD-L1 22C3 IHC assay requests between October 2016 and August 2017. All pathology reports for off-label orders were reviewed for tumor type, site of origin, patient age, sex, and pathologic stage, if available. Results were separated by organ/organ system. Colorectal, esophageal, gastric, pancreaticobiliary, bladder, breast, melanoma and HNSCC cases were further examined for clinicopathologic correlations. Membranous staining in ≥1% tumor cells is considered positive expression for this analysis.

Results: 847/5883 (14.4%) PD-L1 22C3 orders were identified as off-label. Overall off-label PD-L1 positivity was significantly lower than that for NSCLC (40.8% vs. 61.1%, p<0.0001). The most represented off-label orders were on gastrointestinal (GI) tumors (Table 1). Colorectal carcinoma (CRC) represented the most tested tumor type and showed a low frequency of PD-L1 positivity. Squamous cell carcinoma (SCC) of the esophagus was significantly (p = 0.0379) more likely than adenocarcinoma of the esophagus to be positive for PD-L1. Data are presented in detail in Table 2. No significant correlations were found between PD-L1 positivity and patient age, sex, or pathologic stage.

Tumor Origin	Total # Cases	Percent of Total Cases
Gastrointestinal	281	33.2
Genitourinary	60	7.1
Dermatologic	51	6.0
Pulmonary, Small Cell	43	5.0
Head and neck	40	4.7
Breast	37	4.4
Gynecologic	29	3.4
Pleura/peritoneum	20	2.4
Central Nervous System	13	1.5
Soft tissue/bone	11	1.3
Other	17	2.0
Unknown primary	245	28.9

Tumor origin	Total tested	Percent of Off-Label cases tested	Number PD-L1 positive	Percent PD-L1 positive
Colon	91	10.7	11	12.1
Esophagus SCC	16	1.9	12	75.0
Esophagus adenocarcinoma	41	4.8	17	41.5
Stomach	23	2.7	9	39.1
Pancreaticobiliary	27	3.2	5	18.5
Head/neck SCC	23	2.7	14	60.9
Breast	37	4.4	15	40.5
Bladder	37	4.4	18	48.6
Melanoma	35	4.1	25	71.4

Conclusions: GI tumors are most frequently tested for PD-L1 expression. CRC has the lowest incidence of positivity. While the frequency of PD-L1 positivity of melanoma and esophageal SCC is comparable to NSCLC, the overall off-label frequency is significantly lower.

1949 TERT Promoter Mutation and Amplification: A Pan-cancer Study on 20,184 Tumors Profiled by Clinical Genomic Sequencing

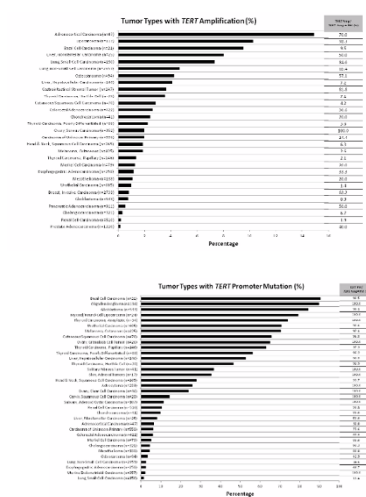
Sounak Gupta¹, Sumit Middha², Ryma Benayed², Maria Arcila³, Ahmet Zehir⁴, Michael F Berger⁵, Marc Ladanyi⁶, Snjezana Dogan⁶. ¹Memorial Sloan Kettering Cancer Center, New York, NY, ²Memorial Sloan Kettering Cancer Center, ³New York, NY, ⁴MSKCC, ⁵Memorial Sloan-Kettering CC, New York, NY, ⁶Memorial Sloan-Kettering, New York, NY

Background: Promoter mutations (PM) involving the *TERT* gene have been identified in multiple cancer types and have been associated with an aggressive clinical course. Mutations in the *TERT* promoter region, at specific sites, leads to the formation of binding sites for the ETS family of transcription factors and this serves as a mechanism for upregulating *TERT* expression. However, the role of *TERT* amplifications (Amp) has not been studied in great detail, and is the focus of the current study.

Design: Mutational profiles of 20,184 tumors analyzed by a hybridization exon-capture next-generation sequencing assay MSK-IMPACT™ were screened for presence of *TERT* alterations.

Results: *TERT* PM were 6.1 times more frequent than *TERT* exonic mutations (2451, 86% vs. 401, 14%) and predominantly involved C>T, C>A and CC>TT substitutions. Tumor types with high frequencies of *TERT* PM (Figure1) included skin cancers (basal cell carcinoma: 90.5%, cutaneous melanoma: 70.4%, squamous cell carcinoma: 65.7%), glioblastoma (84.4%) and myxoid liposarcomas (79%). Overall, PM commonly occurred at position -124 (71%), -146 (23%) and -138 (2%), relative to the transcription initiation site. Primary tumors with *TERT* PM (n=1534), compared to metastatic tumors (n=848) had a significantly higher frequency of alterations at position -124 (1158, 75.5% vs. 541, 63.8%, p<0.0001). Metastatic tumors had a higher incidence of alterations at position -146 (226, 26.7% vs. 308, 20.1%, p=0.0002).

The frequencies of *TERT* Amp in different cancers ranged from 0 to 14.9% (Figure2). Interestingly, in several tumor types, *TERT* Amp was more frequent than *TERT* PM (Figure 1) including liposarcoma (92.3%), small cell lung carcinoma (84.6%), adrenocortical carcinoma (70%), and non-small cell lung carcinoma (65.4%). Conversely, tumors with a high incidence of PM had lower rates of Amp (eg. glioblastoma: 84.4% vs 0.8%, p<0.0001).



Conclusions: Here we highlight the landscape of *TERT* alterations across multiple cancers. Further cancer subtype-specific studies are needed to determine if (1) *TERT* PM at specific sites are associated with relatively more aggressive tumor biology and worse outcomes, and if (2) *TERT* Amp has similar biological significance as *TERT* PM.

1950 Characterization of Biomarkers to Immune Checkpoint Inhibitor Therapy in Solid Tumors

Xiu Huang¹, Meaghan K Russell¹, Angeliki Pantazi², Maria Lvova², Dana Vuzman², Stephen Lyle³, Julie Y Tse³. ¹KEW, Inc., Cambridge, MA, ²KEW, Inc., Lethbridge, AB, ³Univ. of Massachusetts, Worcester, MA, ⁴Tufts Medical Center, KEW, Inc., Boston, MA

Disclosures:

Xiu Huang: *Employee*, KEW Inc.
Meaghan Russell: *Employee*, KEW Inc.
Angeliki Pantazi: *Employee*, KEW Inc.
Maria Lvova: *Employee*, KEW Inc.
Julie Tse: *Consultant*, KEW, Inc.

Background: Immune checkpoint inhibitor (ICPI) therapy has produced durable treatment responses in patients with solid tumors refractory to conventional chemotherapy and targeted therapy. Currently, tumoral expression of programmed death-ligand 1 (PD-L1; CD274) is clinically used as a biomarker of predicted response to immune checkpoint inhibitor therapy in non-small cell lung cancer (NSCLC). However, across solid tumors, only a subset of patients benefit from immune checkpoint inhibitor therapies, so there is a need to identify biomarkers to predict response to such treatment and guide disease management. We investigated the use of large panel next generation sequencing (NGS) to characterize biomarkers to immune checkpoint inhibitor therapy across a spectrum of solid tumors.

Design: NGS and immunohistochemistry (IHC) was performed on a series of solid tumors. NGS analysis included detection of single nucleotide polymorphisms (SNPs), insertions and deletions (indels), copy number variation (CNV), and gene-fusions in 435 cancer-related genes, microsatellite instability (MSI), tumor mutational burden (TMB) based on non-synonymous SNPs, and HPV16/18 and EBV viral status. PD-L1 expression was analyzed by IHC. Genomic alterations in previously reported biomarkers of response to ICPIs were assessed.

Results: 143 solid tumors were analyzed with NGS and PD-L1 IHC. The samples included 80 NSCLC, 15 colorectal carcinoma, 8 cutaneous melanoma, and 6 breast carcinoma. Other tumor types included cervical, ovarian, endometrial, gastroesophageal, pancreaticobiliary, head and neck, urothelial, and prostate carcinoma. The mean TMB varied by tumor type, with melanoma having the highest mean TMB. Approximately half of the cases had PD-L1 expression (equal or greater to 1%), with a higher incidence of expression in NSCLC and melanoma compared to colorectal carcinoma. The relationship between PD-L1 expression and the other biomarkers varied by tumor type (Table 1).

	TMB	KRAS, NRAS, HRAS SNPs	BRAF SNPs	EGFR SNPs	STK11 CNV; MET and ROS1 gene fusions
NSCLC	No association	Positive association	Positive association	No association	No association
CRC	Positive association	No association	Positive association	No association	No association
Melanoma	Negative association	No association	No association	No association	No association

NSCLC: non-small cell lung cancer; CRC: colorectal carcinoma; PD-L1: programmed death-ligand 1; TMB: tumor mutation burden; SNP: single nucleotide polymorphisms; CNV: copy number variation

Conclusions: We characterized biomarkers to immune checkpoint inhibitor therapies across a range of solid tumors. We found tumor-specific differences in the mean TMB and frequency of PD-L1 expression. We also found tumor-specific differences in the associations between PD-L1 and other potential biomarkers, including KRAS, NRAS, HRAS, BRAF, and EGFR mutation status. We found no correlation between PD-L1 expression and MSI and viral status. NGS is an efficient platform for analysis of biomarkers across a range of solid tumors.

1951 PREVIOUSLY PUBLISHED

1952 PREVIOUSLY PUBLISHED

1953 Mutation Spectrum of KRAS Gene in Colorectal Adenocarcinomas using Next Generation Sequencing a Single Institution Large Cohort

Ryan Jones¹, Andrew Bandy², Audrey Deeken-Draisey³, Jie Liao⁴, Leyu Sun⁵, Juehua Gao³, Guang-Yu Yang². ¹Naperville, IL, ²Chicago, IL, ³Northwestern Memorial Hosp, Chicago, IL, ⁴Northwestern University, Chicago, IL, ⁵Northwestern, Chicago, IL

Background: KRAS is one of the most commonly mutated genes in colorectal adenocarcinoma (CRC), affecting approximately 40% of cases. KRAS mutational status has major therapeutic implications regarding the use of anti-EGFR drugs cetuximab and panitumumab. EGFR status assessed by IHC is not predictive of therapeutic effect, however KRAS mutations do predict a lack of response to these drugs. The majority of mutations occur in KRAS codons 12, 13, and 61, however current NCCN guidelines state that patients with any known KRAS or NRAS mutation should not be treated with anti-EGFR therapies. This study aims to identify the spectrum of KRAS mutations, as well as common co-mutations in a large cohort of CRC from a single institution.

Design: Utilizing our institution's clinical CRC cohort, a total of 372 CRC cases have been analyzed using a next generation sequencing (NGS) approach since 2015. NGS was performed targeting 22 cancer-related genes.

Results: Of 372 total CRC cases, 153 harbor a KRAS mutation (41%). Most of these are single base pair substitutions resulting in missense mutations. Purine transitions of G>A substitutions were the most common (56%), followed by the transversions G>T (25%), G>C (8%) and A>T (5%). The majority of these were in codons 12 (70%), 13 (16%), and 61 (8%). Uncommon mutations were identified in codons 146 (n=5), 117 (n=3), 59 (n=2) and 14 (n=1) (Table 1). Three cases had two adjacent nucleotides with alterations (c.180_181TC>AA, p.Q61K; c.36_37TG>CC, p.G13R; c.33_34TG>CT, p.G12C). One case had two separate mutations resulting in mutations in codons 12 and 61. The most frequent coexisting mutation is in TP53 (52%). KRAS mutations appear to be mutually exclusive with BRAF, however there are 3 cases with mutations in NRAS (Table 2).

Mutation	# of cases
p.G12D	48
p.G12V	27
p.G13D	21
p.G12C	10
p.G12S	9
p.G12A	8
p.Q61H	6
p.A146T	4
p.G12R	4
p.Q61L	4
p.K117N	3
p.A59T	2
p.G13C	2
p.A146V	1
p.G13R	1
p.Q61K	1
p.V14I	1
p.Q61R and p.G12V	1

Gene	# of cases
TP53	80
PIK3CA	42
SMAD4	22
FBX7	13
MET	11
PTEN	5
STK11	5
FGFR3	4
NRAS	3
CTNNB1	3
ERBB4	2
ERBB2	1
ALK	1
EGFR	0
BRAF	0
AKT1	0
MAP2K1	0
DDR2	0
NOTCH1	0
FGFR1	0
FGFR2	0

Conclusions: These data show that the rate of KRAS mutations in CRC at our institution is consistent with the reported literature (~40%). However, the high variability in mutations suggests that there may be mutations in KRAS that behave differently than others, especially in the less studied codons such as 146, 117, 59, and 14. The significance of these mutations is not yet fully understood, and may be of prognostic or predictive value. Coexisting mutations in TP53 in more than half of the cases implies chromosomal instability, and there are several other genes of interest that occur with KRAS which may lead to further refinement of our knowledge of the molecular biology of CRC.

1954 Cancer Testis Antigen PRAME Is Abundantly Expressed in Metastatic Melanoma and Other Malignancies

Achim Jungbluth¹, Denise Frosina², Miriam Fayad², Cecilia Lezcano², Klaus Busam³. ¹MSKCC, New York, NY, ²Memorial Sloan Kettering Cancer Center, ³Memorial Sloan-Kettering CC

Background: CT antigens (CTAs) such as NY-ESO-1, MAGE, and CT7 are named after their characteristic expression pattern since they are found in various types of cancer and in normal adult tissues solely in testis. CT antigens are highly immunogenic and due to their limited expression in normal tissues, are employed as vaccine targets for cancer immunotherapy. PRAME (Preferentially expressed Antigen of Melanoma) is another CTA which was identified in a melanoma patient. Interestingly, little is known about the in-situ expression of PRAME. Only recently, suitable reagents for the analysis of PRAME in formalin-fixed paraffin embedded tissues (FFPE) have become available. Consequently, in the present study, we analyzed the presence of PRAME by IHC in normal tissues as well as in a wide variety of tumors.

Design: Several commercially available monoclonal antibodies (mAbs) were tested as to their usability for IHC in FFPE tissues. IHC was done on an automated Leica-Bond stainer platform. Specificity was analyzed in pellets of various cell lines with known PRAME mRNA expression levels. The IHC protocol was optimized and panels of normal tissues as well as tumors were analyzed.

Results: MAb EPR20330 (Abcam, #219650) worked best in IHC and immunostaining was congruent with PRAME mRNA expression in cell line pellets. No staining was present in normal adult tissue except testicular germ cells. PRAME expression in tumors was exclusively nuclear and as follows: Melanoma (metast.): 37/40 (93%); Colorectal Ca: 0/10; RCCs (clear cell): 1/15 (15%); NSCLCs: 12/30 (40%); Hepatocellular Ca: 1/10; Serous ovarian Ca.: 11/20 (55%); Invasive ductal breast Ca.: 7/15 (45%); Synovial sarcoma: 10/10; Myxoid liposarcoma: 5/5; Mesothelioma: 0/10.

Conclusions: The present study is the first comprehensive in-situ analysis of PRAME expression in normal and neoplastic tissue. PRAME shows the typical eponymous CTA expression pattern. However, the extensive and homogeneous presence in metastatic melanoma surpasses other CTAs such as MAGE or NY-ESO-1. High PRAME expression was also found in serous ovarian carcinomas and NSCLCs. All tested synovial sarcomas and myxoid liposarcomas were also positive, similar to other CTAs. Interestingly, little expression was present in colorectal and renal cell carcinomas as seen in other classical CTAs. The high incidence and homogeneous expression indicates that PRAME may be a useful target for vaccine-based immunotherapy of a wide variety of malignant neoplasms, especially metastatic melanoma.

1955 Mismatch Repair Immunohistochemistry to Identify Microsatellite Instability in Solid Tumors

Christine Kim¹, Mohamed Mokhtar Desouki¹, Chanjuan Sh², Jaclyn C Watkins³. ¹Vanderbilt University Medical Center, Nashville, TN, ²Vanderbilt University, Nashville, TN, ³Vanderbilt University Medical Center, Nashville, TN

Background: The recent approval of pembrolizumab, a PD-1 inhibitor, for treatment of advanced solid tumors that are microsatellite instability-high (MSI-H) or mismatch repair deficient (dMMR) has led to an increase in clinical requests for MMR IHC on non-endometrial (EM), non-colorectal (CR) solid tumors. However, experience with MMR IHC protocols in such solid tumors is limited, especially in non-Lynch Syndrome (LS)-type malignancies.

Design: All non-EM, non-CR solid tumor cases with MMR IHC (MSH2, MSH6, MLH1, and PMS2 proteins) performed at clinical request from 2012 onward were included. Tumor H&Es and MMR IHC were reviewed, and MMR patterns of expression were noted. Family history, past medical history, and genetic testing results were abstracted from the medical record.

Results: 19 non-EM, non-CR solid tumors with MMR IHC were identified. 13 tumors (68.4%) were LS-type malignancies, including adrenocortical carcinoma (ACC, n=3), urothelial carcinoma (n=1), anaplastic astrocytoma (n=1), sebaceous neoplasms (n=2), pancreaticobiliary adenocarcinoma (ACA) (n=4), duodenal ACA (n=1),

and gastric ACA (n=1). Non-LS-type tumors (n=6, 31.6%) included uterine spindle cell sarcoma, NOS (n=1), cervical carcinosarcoma (n=1), embryonal rhabdomyosarcoma (n=1), MPNST (n=1), breast carcinoma (n=1), and esophageal ACA (n=1). Of the 19 tumors, 4 (21%) were dMMR, all of which were LS-type malignancies. 1 ACC, arising in a 37-year-old female, demonstrated complete loss of MSH2 and MSH6. Germline testing was negative for this patient. An ACC in a 68-year-old male demonstrated patchy loss of MSH6 and complete loss of MSH2. The patient had a germline MSH2 deletion. A duodenal adenocarcinoma arising in a 69-year-old male and a sebaceous neoplasm in a 76-year-old male both demonstrated loss of MSH6 and MSH2. Neither patient received genetic testing.

Conclusions: Requests to test non-EM, non-CR solid tumors for MSI via MMR IHC are becoming increasingly common. Our experience suggests that non-EM, non-CR solid tumors that are dMMR are likely to be LS-related. Therefore, in institutes that commonly test non-EM, non-CR solid tumors for MSI or MMR deficiencies, access to genetic testing and counseling, as appropriate, are necessary. Further, our preliminary evidence suggests that screening historically non-LS-type malignancies may be relatively low yield. Future steps include collecting additional cases prospectively and evaluating unusual staining patterns (e.g., clonal loss) as they arise.

1956 A Newly Licensed Peptide Presenter HLA-F: the Occurrence and the Prognostic Significance of this Cancer Immunoeating Molecule in Renal Cell Carcinoma and its Occurrence in Glioblastoma

Leos Kren¹, Katarina Muckova², Vaclav Kubes², Filip Sokol². ¹University Hospital Brno, Brno, Czech Republic, ²University Hospital Brno

Background: Among cancer immunoeating non-classical human leucocyte antigens (HLA) class II, HLA-F remains to be the most enigmatic. Originally it was thought to be specifically expressed only by extravillous trophoblast, which indicated its physiological role in a development of maternal tolerance to a semiallogeneic fetus (via engagement with inhibitory receptors on NK cells, mechanism also adopted by cancer cells to bypass host immunity). The expression by trophoblast was recently confirmed (Hackmon R 2017). Moreover, recently a peptide presenting function (presentation of peptides of unconventional length) was described in HLA-F (Dulberger CL 2017). Renal cell carcinoma (RCC) is characterized by its immunogenicity. Glioblastoma (GB) is a malignancy of an immune privileged site. An expression and prognostic significance of HLA-F by neoplastic cells in RCC and the expression in GB is not characterized.

Design: We evaluated the expression of HLA-F specific mRNA transcripts produced by neoplastic cells in 73 cases of RCC and in 54 samples of normal kidney parenchyma. We also evaluated expression of HLA-F molecule immunohistochemically in a pilot study of 24 cases of GB (IDH-wildtype in accordance with WHO 2016 revision). The results in RCC were statistically correlated with several clinicopathological parameters.

Results: We revealed that HLA-F is up-regulated in RCC (Tab.). On the other hand, its up-regulation is counterintuitively associated with prolonged disease-free survival (Fig. 1), more favorable pT stage and lower nuclear Fuhrmann's grade. In the pilot study of GB, we found cytoplasmic expression of HLA-F (Fig. 2) in 10 cases (42%). Because of a possibility of aberrant activation of expression of non-classical HLA molecules by interferons, the identification of HLA-F status could contribute to better selection of patients with RCC who could possibly benefit from more tailored neoadjuvant biological/immunological therapy. This molecule could represent useful prognostic biomarker in RCC.

	Non-paired samples			Paired samples		
	RCC	adjacent non-tumor renal parenchyma	p-value	RCC	adjacent non-tumor renal parenchyma	p-value
	n= 73	n=54		n=54	n=54	
25% Percentile	0,10865	0,0320365		0,096858	0,0320365	
50% Percentile	0,189213	0,0382799	p < 0,0001	0,1773	0,0382799	p < 0,0001
75% Percentile	0,348363	0,0545022		0,31995	0,0545022	

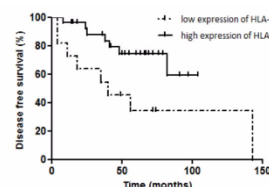
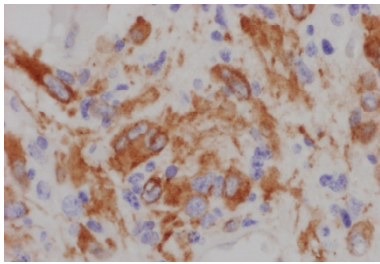


Fig. 1 Disease-free survival of RCC patients according progression (cut off value = 0.1293, p = 0.0226, *, Long-rank test).



Conclusions: Non-classical molecule HLA-F, recently proven to be a peptide presenter, physiologically protects the fetus from maternal allorecognition. Our results suggest its role in cancer immunoevasion in RCC and we proved its cytoplasmic expression in 42% of cases of GB. Further studies appear warranted. This publication was written at Masaryk university as part of the project MUNI/A/1405/2016. Also supported by Ministry of Health CZ - DRO (FNBr, 65269705), AZV/ Czech Health Council grant 17-32758A.

1957 Serum miR371a Quantitation for Assessing Tumor Burden in Testicular Germ Cell Tumors

Christian Kunder¹, Yoriko Imae², Sandy Srinivas², Alice C Fan². ¹Stanford University School of Medicine, Stanford, CA, ²Stanford University Medical Center

Background: Existing circulating biomarkers for testicular germ cell tumors (TGCTs) (primarily alpha-fetoprotein; AFP and beta-human chorionic gonadotropin; bHCG) are insensitive for low levels of residual disease and are not elevated in every patient with a TGCT. As a result, clinicians are forced to rely heavily on imaging modalities that lack specificity.

miR371a-3p is present in a cluster of miRNAs that is highly overexpressed in almost all TGCTs compared to normal tissues, and it is easily measurable in serum using quantitative reverse transcriptase polymerase chain reaction (RT-qPCR).

Design: To test the usefulness of this biomarker, we collected serial sera from nine patients about to begin treatment for metastatic TGCT, three patients about to undergo orchiectomy, and seven patients without TGCT. Most patients had mixed germ cell tumors at orchiectomy, but the cohort also included three patients with pure seminoma, one with pure embryonal carcinoma, and one with pure teratoma. For quantitation, we extracted cell-free RNA and then performed qPCR. We also measured levels of an exogenous miRNA (*Caenorhabditis elegans* miR-39-3p) added to serum sample in controlled quantities prior to RNA extraction, as well as of another human miRNA (miR-20a-5p) that is present at high levels in human serum and has been suggested as a "housekeeping" miRNA.

Results: Serum miR-371a-3p was elevated in twelve of fourteen patients with known active disease (either metastatic or pre-orchiectomy). An additional patient with a central nervous system germinoma was also positive. The negative cases included one pre-orchiectomy patient with a 1.3 cm pT1 pure seminoma and one patient with metastatic germ cell tumor (mixed histology at orchiectomy). The one case of pure teratoma was positive. Levels of miR371a-3p tracked with disease burden and correlated with canonical biomarkers when these were elevated. Three patients without elevated AFP or bHCG had elevated miR371a-3p. Seven of eight patients without TGCT had undetectable miR371a-3p levels, and the eighth had a very low level.

Conclusions: Serum miR371a is an extremely promising biomarker for testicular (and possibly other) germ cell tumors, including those without elevated canonical biomarkers. It has the potential to greatly improve tumor burden assessment and monitoring, as well as for aiding primary diagnosis in patients with testicular masses. More extensive studies to establish the dynamic range of this test and its sensitivity and specificity are required.

1958 The Functional Roles and Applications of Adenylate Kinase AK1-AK4 Signatures in Human Lung Adenocarcinomas

Tsung-Ching Lai¹, Michael Hsiao², Yi-Hua Jan³. ¹Academia Sinica, Taipei, ²Academia Sinica, ³Genomics Research Center, Academia Sinica

Background: In our previous study, we found adenylate kinase 4 (AK4) highly correlates to the tumor malignant progression of lung adenocarcinoma and promotes metastasis. However, the interplay among AK isoforms and their impact on lung cancer pathogenesis remains unclear.

Design: The expression patterns of AK family in lung cancer cell lines and clinical patient cohort (TCGA) were determined. The major upstream regulators from the analysis of AK signatures analyzed by

IPA were confirmed in clinical lung cancer tissue arrays. The molecular validations were determined with functional promoter assay, qPCR analysis, and migration/invasion assays. Further applications of AK1/AK4 for lung cancer therapy were also determined.

Results: In this study, we found that AK1 and AK4 have reversed correlation in lung adenocarcinoma cohort in TCGA and the clinical tissue microarray. The expression of AK1-AK4 signature was correlated to the poor progression, recurrence and worse chemotherapeutic outcome. From the IPA upstream analysis of the AK1-AK4 signatures, TBX2, TTF-1 and p53 were found to be playing the major roles. By modulating the expression AK1 and AK4, we would see the correlative response of these regulators by promoter assay. Cells would also reduce the mobility with the downregulated activity of upstream regulators. In the other hands, AK4 was found associated with the EMT. Since EMT was reported as a factor to cause the resistance to the chemotherapy. We also tested the combinational effects of AK1/AK4 with the selected chemotherapeutic compounds in lung cancer cells.

Conclusions: Our study depicts the new role of AK1-AK4 signature in lung adenocarcinomas. We also discovered the dominant transcriptional factors in this pathway. The interactions lead to the poor progression and metastasis in clinics and may create a novel strategy for effective chemotherapy responses in lung cancer patients.

1959 Molecular Characterization of Aggressive Estrogen Receptor Positive Breast Cancer Resistant to Palbociclib Therapy

Li Lei¹, Chieh-Yu Lin², David Steiner³, James M Ford⁴, James L Zehnder⁵, Carlos J Suarez². ¹Stanford University, ²Stanford University Medical Center, Stanford, CA, ³Stanford University School of Medicine, ⁴Stanford University, ⁵Stanford University

Background: Approximately 80% of breast cancers are hormone receptor positive. Endocrine therapies are the mainstay of the treatment for these patients and it substantially reduces the relapse rate. However, some patients still relapse during or after completing treatment. The addition of palbociclib, a CDK4/6 inhibitor, to endocrine therapy could provide clinical benefit to 34% of treatment resistant patients (Turner, N Engl J Med, 2015). However, no molecular biomarker or profile has been identified to guide palbociclib therapy. The aim of this study is to molecularly characterize estrogen receptor (ER) positive breast cancer resistant to palbociclib in order to recognize molecular features that could be predictive for palbociclib therapy.

Design: ER-positive breast cancer cases discussed on the institutional molecular tumor board in 2017 were reviewed. Cases with a history of resistance to palbociclib and targeted tumor sequencing data available were collected.

Results: Two ER positive, HER2 negative, Ki-67 high, invasive ductal carcinoma met the inclusion criteria. Both cases demonstrated multiple chromosomal alterations. Case 1 showed amplification of multiple genes on chromosomal regions 11q13, 20q11-13 and 12q15, along with *CHEK2* loss of exons 8-15 and a *PIK3CA* H1047L mutation. Case 2 showed amplification of genes on 11q13, 8p11, 8q24, 1q32 and 12q15, in addition to *PTEN* loss and an *SLIT2* Q598fs mutation. Between these two cases, copy number gains on 11q13 and 12q15 were shared. Even though *CCND1* is on chromosome 11q13 and *CCND1* amplifications have been speculated to be targetable by palbociclib, our cases suggest that they are instead resistant to palbociclib. Moreover, the 11q13 alteration has been described as the hallmark of Integrative Cluster 2, a molecular subgroup of breast cancers that was recently generated using multiple genomic views (Curtis, Nature, 2012). Breast cancers in this subgroup are mainly luminal tumors with poor prognosis and are hypothesized to be driven by a cassette of genes on 11q13/14 rather than a single oncogene. Our cases support that when a single gene "amplification" is part of a larger chromosomal amplification it might not be targetable as expected.

Conclusions: Copy number gains on 11q13, a distinctive feature of the Integrative Cluster 2 molecular subgroup, may be a predictive biomarker for lack of response to palbociclib in aggressive ER-positive breast cancer. More cases, including those responded to palbociclib, are necessary to confirm this finding.

1960 Importance of Molecular Analysis of BRCA1 and BRCA2 Genes in Gynecological Neoplasms. Descriptive Study of 144 Cases

Sara Marcos¹, Irene Alconche², Laura Ferreira², Ainara Azueta³, Javier Freire⁴, Maria Pilar Garcia-berbe⁵, Carmen Hinojo², José-Javier Gómez-Román². ¹HUMV/IDIVAL, Santander, Cantabria, ²HUMV, ³HUMV/IDIVAL, Santander, Cantabria, ⁴IDIVAL, Santander, Cantabria, ⁵IDIVAL, Santander

Background: Hereditary breast and ovarian cancer syndrome (HBOCS) is a status that increases the likelihood of developing breast, ovarian and other cancers due to the presence of germline mutations in BRCA1 or BRCA2 genes located in chromosome 17q21 and 13q12/13 respectively. Between 5 and 15% of breast and ovarian cancers

are hereditary.

In breast cancer, up to 50% of the cases are due to mutations in BRCA1 and 40% in BRCA2. In ovary cancer, 90% have mutations in BRCA1 and 5-10% in BRCA2.

Design: We described our results of BRCA1 and BRCA2 molecular genetic analysis since 2015 until now, through lymphocyte DNA analysis by of Next Generation Sequencing (Multiplicom and Sophia DMM bioinformatic analysis) in MySeq Illumina platform and detection of large deletions in both genes by MLPA.

Results: A total of 142 women and two men with breast and/or ovarian cancer, aged between 27 and 81 years, with a mean of 55 years, are studied. Of these, 101 had a family history of multiple neoplasms: 73 breast, 6 ovary and 22 of both cancers. The remaining 43 patients had no family history.

From the analysis carried out, sixteen patients presented genetic alterations in BRCA1 (11%) and ten in BRCA2 (7%) (see fig 1).

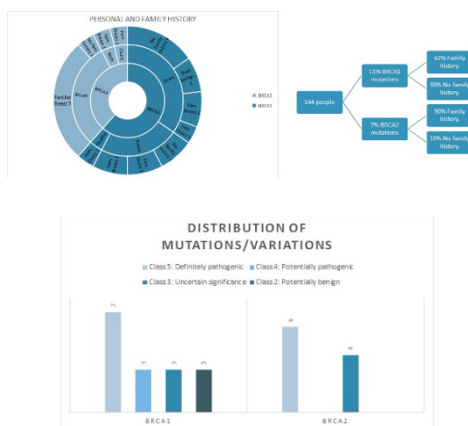
The patients with ovarian cancer had a mutation rate of 18% and those with breast cancer of 15%.

In the case of BRCA1, seven definitive pathogenic mutations (class 5) are observed, and in BRCA2, six mutations of class 5 (see fig 2).

One of the variants found in exon 11 of BRCA1, class 5, c.2902_2903insTC, p.Pro968Leufs, rs398122670 is described with geographic aggregation in families from the north of Spain.

The variant c.68_69delAG (p.Glu23Valfs) in exon 2 of BRCA1 rs386833395 (also known as 185delAG or 187delAG) is one of the three founding pathogenic variants in the Askanazi Jewish population of origin.

Two cases show extensive heterozygous deletion in exons 1 to 13 of BRCA1 and exons 3 to 11 of BRCA2.



Conclusions: With the molecular analysis of the HBOCS, directed programs of early detection, prevention and genetic counseling have been established in our community.

The importance of the molecular analysis of the BRCA1 and BRCA2 genes has also a predictive role for the selection of patients susceptible to treatment with Olaparib in high grade ovarian carcinoma with BRCA germline mutation as maintenance after failure of three or more lines of chemotherapy. In our series, a patient is pending treatment.

1961 Co-Occurrence of TP53 and CDKN2A Genomic Alterations is Less Common in HPV-Associated Squamous Cell Carcinomas

Lopa Modi¹, Aditya S Kuvadekar², Eli Balshan³, Hua Zhong⁴.
¹Hillsborough, NJ, ²Saint Barnabas Medical Center, West Orange, NJ, ³Saint Barnabas Medical Center, ⁴Monmouth Medical Center

Background: Deregulations of tumor suppressor genes p53 and Rb is a fundamental mechanism of carcinogenesis. Inactivation of CDKN2A (cyclin-dependent kinase inhibitor 2A) can exacerbate the disruption in these two pathways. Prior studies have shown that TP53 gene is the most commonly mutated gene in human cancers. CDKN2A mutations have been identified in a subset of human squamous cell carcinomas (SCCs). Co-existing genomic alterations of these two tumor suppressor genes may accelerate the disruption of cell cycle control and can lead to SCC carcinogenesis/tumor progression.

Design: The FoundationOne NGS panel was employed to analyze eighteen (18) formalin-fixed, paraffin-embedded specimens of late-stage primary or metastatic SCC of multiple organs including seven from anus, one from vagina, one from tonsil, six from skin and three from lung. Out of eighteen, nine cases were HPV-associated SCC including seven from the anus, one from the vagina, and one from the tonsil. Available large-scale cancer genomics data sets on cBioPortal with a focus on squamous cell carcinomas (SCC) were analyzed.

Results: Concomitant TP53 and CDKN2A genetic alterations (predominately mutation or deletion) were found in 38% (7/18) of all specimens tested. Conversely, only two of the nine (22%) HPV-associated SCCs showed concomitant TP53 and CDKN2A alterations. Five out of nine (56%) of the non-HPV-associated SCCs showed concomitant TP53 and CDKN2A alterations. The cBioPortal (9-23-2017) query of the seven SCC data sets (1,167 cases) found that the average co-occurrence of TP53 and CDKN2A mutations is 21% (250/1,167) in total. The co-occurrence is 38% (11/29) in skin, 36% (64/178) in lung, 33% (167/504) in head and neck SCCs, and only 0.9% (2/231) in the HPV-related SCCs (uterine, cervix, and oral) and 2.7% (6/225) in esophageal SCC (2 data sets). In general, TP53 is more frequently mutated than CDKN2A. CDKN2A mutation, if present, tended to coexist with TP53 mutation.

Conclusions: Simultaneous TP53 and CDKN2A mutation, which enhances tumor progression, appears to be infrequent in HPV-related SCCs as compared to non-HPV-related SCC. Further research is necessary for determining its value as a prognostic indicator.

1962 Evaluation of the Impact of Targeted Assays in Tailoring Cancer Treatment

Silvia Morales¹, Gemma Toledo¹, Raquel Bratos¹, Gema Moreno¹, Mar Lopez Colomer¹, Pablo Garcia Sanz¹, Pilar Lopez Criado¹, Alejandro Rojo¹, Juan F Garcia¹.
¹MD Anderson Cancer Center Madrid, Spain

Background: Describe a single-center experience with comprehensive genomic profiling (CGP) to identify genotype directed therapy (GDT) options for patients with malignancies regardless of the primary disease site or cancer type. We have two NGS platforms: Lung/colon cancer panel (analyzing 90 regions in 22 genes) and general cancer panel (207 regions in 50 genes).

Design: Patients who had CGP by our laboratory between January 2012 and August 2017 were included. The medical records were analyzed retrospectively. The objectives of this study were to determine the proportion of patients who benefited from GDT, and to identify barriers to receiving GDT.

Results: A total of 214 adult patients with a histologically confirmed diagnosis of malignancy were included. A total of 162 (75%) patients had genomic alterations and 118 (55%) were candidates for GDT. Only thirty patients (14%) modified their treatment, based on this results. CGP revealed potential treatment options in 61% of patients profiled. However, multiple barriers to therapy were identified, and only a small minority of the patients derived benefit from GDT.

Conclusions: CGP revealed potential treatment options in 61% of patients profiled. However, multiple barriers to therapy were identified, and only a small minority of the patients derived benefit from GDT.

Co-funded by the National Institute of Health Carlos III (ISCIII) and European Regional Development Fund (FEDER) (PT13/0010/0010).

1963 Extracellular Vesicle Imaging and Isolation by High Resolution Flow Cytometry

Terry Morgan¹, Carmen Winters².
¹Oregon Health Science Univ, Portland, OR, ²OHSU, Portland, OR

Background: There is intense interest in developing new methods to perform liquid biopsies of tumors using blood samples. This is possible because tumors release millions of lipid encapsulated extracellular vesicles (EVs)/ml into the blood stream. The term EVs includes small exosomes (50-150 nm) and larger sub-micron sized microvesicles. Progress in the field has limited, however, by the lack of cell and size-specific rapid isolation methods. To address this issue, our group has developed a new multiparametric high resolution flow cytometry (HRFC) sorting method that can reliably identify, quantitate, and purify cell- and size-specific EVs from any tumor of interest. In this study, we investigated whether we could visualize and purify ovarian neoplasm-related EVs from patient plasma (n=110 cases) compared with negative controls (n=78 males or young women).

Design: FITC-conjugated submicron-sized polystyrene beads (100, 160, 200, 240, 300, 500, 900nm) were used as sizing and sorting efficiency controls and imaged using a FACsAria Fusion (BD Biosciences) with settings and reagents optimized for HRFC. Platelet-related CD41+ and CD9+ EVs present within all plasma samples served as internal positive controls. All samples were standardized relative to collection (EDTA tubes), processing, banking at -80, staining times, and dilution into normalized 0.1um PBS buffer containing uniform numbers of 200nm beads that serve as a uniform denominator between samples. In this pilot study, plasma from women with high stage adnexal papillary serous carcinoma were stained for CA125-PE and EpCAM-FITC. Only EVs that co-expressed these markers were considered true positives. All test samples were run in triplicate. Sorted EVs were prepared for electron microscopy, nanoparticle tracking analysis (Nanocyte), and-omics comparisons.

Results: Cell- and size-specific EVs can be resolved and sorted to

a high level of purity (>99%) using as little as 100 ul of plasma to generate isolated EVs (10⁶/ml) within minutes. In this pilot study of high stage ovarian serous carcinoma cases CA125/Epcam+ EVs represented 1.42-1.88% of the total nanosized population (~10⁷/ml); whereas, negative control plasmas were reproducibly negative with 0.08-0.10% of total events in the same volume of plasma. Electron microscopy confirmed sorted EVs were the expected size, purity, and Nanocyte further confirmed relative size and concentration.

Conclusions: HRFC is a new approach to visualizing and isolating cell- and size-specific EVs.

1964 Pan-Cancer Detection of Mismatch Repair Deficiency using Targeted Massively Parallel Sequencing

Jonathan A Nowak¹, Fei Dong², Alexander Frieden³, Priyanka Shivdasani¹, Leah Bialic⁴, Jacqueline L Bruce², Vanesa Rojas-Rudilla², Christine Bertrand¹, Matthew D Ducar¹, Frank Kuo⁵, Neal Lindeman⁶, Laura E MacConaill¹, Lynette Sholff¹. ¹Brigham and Women's Hospital, ²Brigham and Women's Hospital, Boston, MA, ³Dana Farber Cancer Institute, Boston, MA, ⁴Dana-Farber Cancer Institute, ⁵Brigham & Women's Hospital, Boston, MA, ⁶Brigham and Women's Hospital Pathology, Boston, MA

Background: Determination of mismatch repair (MMR) pathway status has specific clinical implications for several tumor types, and, more broadly, can help identify patients that may benefit from therapy with checkpoint blockade inhibitors. This study aimed to determine the feasibility of using mutational patterns in targeted, massively parallel sequencing data to predict MMR pathway status across a wide variety of tumor types undergoing routine testing.

Design: Tumors were analyzed by a massively parallel sequencing assay that interrogates 447 cancer-associated genes for mutations, copy number variations and structural alterations. Multiple measures of DNA mutational patterns were calculated for each tumor, including the number of small insertion/deletion events that occur in homopolymer regions per megabase of exonic sequence data and the overall mutational burden per megabase. Immunohistochemistry for MMR protein expression or PCR for microsatellite instability were performed to orthogonally define MMR status for each tumor. A training set comprised of different cancer types with a broad range of frequencies for MMR deficiency was used to define thresholds that optimally identified MMR-deficient tumors.

Results: MMR deficiency, as assessed by standard criteria, was present in 14.2% (48 of 337) of tumors in the training set, spanning 12 different cancer types, including gastrointestinal (27 of 264) and non-gastrointestinal (21 of 73) tumors. MMR-deficient tumors had a significantly higher overall mutational burden (p<0.001) and a higher burden of insertions/deletions in homopolymer regions (p<0.001), regardless of tumor type. A threshold of > 1.5 insertions/deletions in homopolymer regions per megabase optimally classified cases in the training set, yielding a sensitivity of 97.9% and specificity of 98.0%. These performance characteristics were maintained in tumors with low neoplastic content (10-20%) and in tumors with low sequencing coverage depth (100-250x). This approach successfully detected MMR deficiency in tumors with *MLH1* promoter methylation, and both germline and somatic mutations in the core MMR pathway genes.

Conclusions: Our findings demonstrate that DNA mutational pattern, as assessed by a targeted sequencing panel, can serve as an accurate predictor for MMR pathway status across a broad variety of tumor types. Such an approach can help streamline existing molecular testing for MMR deficiency and can enable efficient screening of many tumor types for MMR deficiency.

1965 Detection of Diverse Mutational Signatures using Targeted Massively Parallel Sequencing

Jonathan A Nowak¹, Ryan Schmidt¹, Jessica Posada¹, Fei Dong², Alexander Frieden³, Priyanka Shivdasani¹, Leah Bialic⁴, Matthew D Ducar¹, Neal Lindeman⁵, Laura E MacConaill¹, Frank Kuo⁶, Lynette Sholff¹. ¹Brigham and Women's Hospital, ²Brigham and Women's Hospital, Boston, MA, ³Dana Farber Cancer Institute, Boston, MA, ⁴Dana-Farber Cancer Institute, ⁵Brigham and Women's Hospital Pathology, Boston, MA, ⁶Brigham & Women's Hospital, Boston, MA

Background: Somatic tumor alterations may be caused by numerous distinct mutagenic processes, many of which generate specific DNA damage patterns. Several groups have demonstrated that massively parallel sequencing (MPS) can be used to detect clinically important mutational signatures such as mismatch repair (MMR) deficiency. This study aimed to determine whether other mutational signatures with potential clinical relevance could be detected by targeted MPS and how their presence correlates with exposure to relevant mutagenic processes.

Design: Tumors were analyzed by a locally-developed MPS assay that interrogates 447 cancer-associated genes. Using published signatures derived from whole exome sequencing, we developed an algorithm for our targeted assay that analyzes mutational patterns

in tumors with an elevated mutation burden (≥12 variants/Mb) to detect the presence of DNA damage due to UVA light exposure, tobacco smoke exposure, prior treatment with alkylating agents (temozolomide), impaired *POLE* DNA polymerase function, and APOBEC enzyme dysregulation. The algorithm was further refined using published targeted exome sequencing data and its performance evaluated against clinicopathologic features documented for each tumor, including origin at a sun-exposed site, smoking history, prior treatment with temozolomide or concurrent *POLE* hotspot mutation.

Results: Of ~4000 total tumors tested, 778 had ≥12 variants/Mb and mutational signatures were detected in 41% of these. MMR (n=116), tobacco (n=107) and UVA (n=49) signatures were the most common. Relative to clinicopathologic features, specificity for detection of tobacco, UVA, temozolomide, and *POLE* signatures ranged from 97-100%. No specific clinical correlate was identified for APOBEC signature, however this was enriched, as expected, in bladder, breast, lung, and HPV+ tumors. Sensitivity ranged from 46% for temozolomide to 82% for UVA.

Conclusions: Numerous mutational signatures can be reliably detected via targeted MPS. More than 40% of tumors with an elevated mutational burden exhibit an identifiable mutational signature by this approach. Specificity for individual mutational processes, as assessed by clinicopathologic correlates, is generally excellent, while sensitivity is more variable. The ability to detect diverse mutational signatures using a routine sequencing assay can provide diagnostic utility and may enhance our understanding of tumor biology.

1966 A Possible New Way of Dividing Cervical HSIL Based on the Presence of Diffuse -Type Signal in Dysplastic Epithelium Using HPV DNA or mRNA In Situ Hybridisation Study

Ondrej Ondic¹, Jana Němcová², Katerina Cerna³, Reza Alaghebandan⁴. ¹Biopsticka Laborator s.r.o., Pilsen, ²Biopsticka laborator, s.r.o., Pilsen, Czech Republic, ³Biopsticka laborator s.r.o., ⁴Royal Columbian Hospital, New Westminster, BC

Background: Cervical HSIL are stable lesions that for most part are unlikely to progress to carcinoma. But HSIL lesions associated with active production of intracellular/intranuclear HPV mRNA are deemed to be transforming lesions with higher risk of progression to carcinoma. Currently the distinction between "low - risk" and "high - risk" HSIL may not be possible. In situ hybridisation (ISH) HPV DNA studies have shown that there were two types of ISH signals in the nuclei of cervical squamous dysplastic epithelium namely dotted type of signal (correlating with low nucleic acid copy number) and diffuse nuclear signal (correlating with very high nucleic acid copy number). The aim of the study is to evaluate performance of ISH methods (DNA vs mRNA) and to interpret ISH signal presentation in different HSIL lesions in a new way.

Design: The study group consists of 17 consecutive cervical cone biopsies harbouring HSIL lesion and 3 squamous cell carcinomas. HPV detection and typing in representative FFPE were carried out. HPV DNA ISH was performed using the BenchMark automated slide staining system (Ventana Medical System) and the INFORM HPV III Family 16 Probe (B) set and iViewBlue plus detection kit (Roche). Punctate or diffuse nuclear staining was scored as positive. HPV RNA ISH was performed using RNAscope HPV-test (Advanced Cell Diagnostics) with HPV-HR18 probe on automated system Discovery Ultra by Ventana Medical systems. The RNAscope ISH signal was identified as strong clear punctate chromogenic dots present in the nucleus and/or cytoplasm.

Results: Strong (dotted-type) HPV mRNA ISH signal was present in all 20 studied lesions. Peculiar strong diffuse-type HPV mRNA ISH signal was detected in the most superficial cells of HSIL lesion in 8 cases. This correlated with the presence of diffuse/episomal type of HPV DNA ISH signal. There was no diffuse-type HPV mRNA or DNA ISH signal in the intermediate or basal level of HSIL epithelium or in carcinoma cases.

Conclusions: 1. HPV mRNA ISH is superior to HPV DNA ISH due to the minimal background artefacts and higher number of strong signals. 2. Both DNA and mRNA HPV ISH methods can be used to assess "growth rate" of squamous dysplastic epithelium. 3. This approach may have the potential to assort HSIL lesions into two groups of „slow proliferating“ (with diffuse and dotted-type ISH signal) and „fast proliferating“ HSIL (with dotted ISH signal only), which may ultimately identify HSIL lesions with higher risk of progression toward invasive carcinoma.

1967 Next Generation Sequencing Allows Deeper Analysis of the DNA Mismatch Repair System

Andrei Plagov¹, Sushant A Patil², Sabah Kadr³, Lauren L Ritterhouse², Jeremy Segaf³. ¹University of Chicago, Chicago, IL, ²University of Chicago, Chicago, IL, ³University of Chicago

Background: Microsatellite instability has been shown to play a

major role in the pathogenesis of a variety of cancers and is a result of impaired DNA mismatch repair (MMR) system. It is traditionally tested by a polymerase chain reaction (PCR) based method, using limited number of loci for amplification and matching normal and test samples. Using next generation sequencing for detection of MSI we were able to analyze much higher number of loci and correlate the data with morphology of the tumor.

Design: We performed NGS-based OncoPlus assay on 15 clinical specimens of gastrointestinal tract carcinomas and endometrial carcinomas, with known high status of microsatellite instability (MSI-H). The assay pipeline assessed stability of a locus, for a total 338 homopolymer loci, spanning across the entire territory of the assay. For each locus, reads distribution (normalized to a fraction of locus' total reads) was generated. Then, absolute value of the stepwise difference between that read distribution and normal distribution (generated using normal tissue data) was calculated. A locus was considered unstable if this value was more than three standard deviations of the average value obtained from micro-satellite stable samples distribution. Finally, percent of unstable loci was calculated and plotted against known microsatellite stable samples. Data was correlated with immunohistochemistry results for the MMR proteins, polymerase chain reaction results, and histologic grade of tumor.

Results: Fourteen out of fifteen MSI-H specimens showed high percent of unstable loci, above 30%, and correlated with loss of nuclear staining for MMR proteins in tumor cells and results of polymerase chain reaction. Histologic section of the single case with lower percent of unstable loci, 23%, showed FIGO 1 endometrial carcinoma with background complex endometrial hyperplasia with atypia.

Conclusions: Next generation sequencing for MSI analysis allows deeper analysis of the microsatellite loci with stratification of tumors based on the percent of unstable loci.

1968 Beyond Molecular Tumor Heterogeneity: pelf4E and Protein Synthesis Take Control as Prognostic Factors and Therapeutic Targets

Santiago Ramon y Cajal¹, Jose Castellv², Irene Sansano³, Elena Martinez-Saez, Javier Hernandez-Losa⁴, Nahum Sonenberg⁵, Vicente Peg⁶. ¹Hospital Universitari Vall d'Hebron, Barcelona, ²Vall d'Hebron Univ Hosp, Barcelona, ³Hospital Universitari Vall D'Hebron, Barcelona, Spain, ⁴Hospital Universitari Vall d'Hebron, VHIR, CIBERONC, Barcelona, ⁵McGill University, Montreal, QC, ⁶H.U. Vall d'Hebron, Barcelona

Background: During the last decades the most relevant advances in cancer have been related to the detection of new genetic alterations and therapeutic targets. Although translation of these findings into clinics have allowed increased survival in some types of tumors, expectations remain poor in advanced stage epithelial tumors. Cellular stress caused by hypoxia, lack of nutrients, oxidative species or DNA damage may inhibit signaling factors of the mTOR and ERK1/2 pathways. Because the response to inhibitory agents depends on the expression of their cellular targets pathways, protein expression is proposed as the actual reflection of cellular alterations of tumor cells.

Design: We have performed immunohistochemical studies in more than 2,500 human tumors (breast, lung, ovary, endometrial an colon carcinomas, mesotheliomas, sarcomas, gliomas, melanomas), to analyze the expression and post-translational modifications of key signaling factors for the control of protein synthesis. HER2, ki67, pMAPK, mTor, 4E-BP1, p4E-BP1, eIF4E, pelf4E, and Epithelial-Mesenchymal Transition (EMT) factors (N-cadherin, snail, slug, YB1, pYB1 and vimentin,) were assessed by specific antibodies in whole paraffin sections. A homogeneous and diffuse pattern was considered when >80% tumor cells displayed a strong positivity. Levels of expression were semi quantitatively evaluated as percentage and intensity of stained tumor cells (histo-score [H score]) and correlations analyzed by using Kruskal-Wallis and Kaplan-Meier (log Rank) statistical tests.

Results: Of the several studies performed, we observed that the expression of p4E-BP1 and pelf4E correlated with worse prognosis. In addition, pelf4E usually exhibited homogeneous expression in tumors in contrast to the patched and heterogeneous appearance of pMTOR, pERK1/2 and pS6.

Conclusions: The intense and homogenous expression of pelf4E due to upstream oncogenic alterations and by p38 activation after cellular stress, points to this factor as a good therapeutic target. Noteworthy, inhibitors of the kinase phosphorylating eIF4E are showing promising clinical results when applied alone or in combination with others therapeutic approaches, such as antiPDL1 therapies. This studies also highlight the importance of the study of protein expression in histological sections beyond genomics in human tumors.

1969 Resolving HER2 Discrepancies in Breast Cancer Using Genomic Profiling

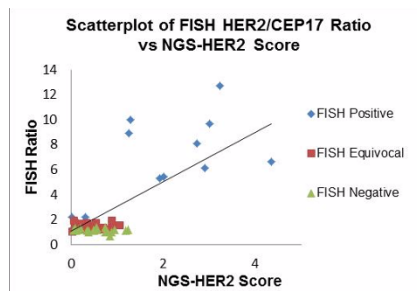
Rongqin Ren¹, Dan Jones², Weiqiang Zhao³, Peng Ru⁴, Kristin Miller⁴, Sean Caruthers⁴, Jordan B Evans⁵. ¹Ohio State University

Wexner Medical Center, Westerville, OH, ²The Ohio State University, Columbus, OH, ³Ohio State University, Columbus, OH, ⁴Ohio State University, ⁵Ohio State University, Columbus, OH

Background: HER2 activation in breast cancer is used to determine the application of anti-HER2 therapy. Immunohistochemistry (IHC) and fluorescent *in-situ* hybridization (FISH) are two traditional methods to assess HER2 status, but they can produce equivocal or discordant results in up to 15% of cases. Studies have demonstrated that equivocal/borderline FISH and IHC results are difficult to reconcile and show variable correlation with clinical outcomes with trastuzumab. Next-generation sequencing (NGS) designed as cost-efficient panels can also give other needed genetic data. In this study, we have validated the clinical application of NGS as an alternative method to resolve HER2 equivocal or discordant results by more accurate measurement.

Design: Breast carcinoma cases with concurrent IHC and FISH studies were randomly selected to include 38 concordant cases, 21 discordant and 13 equivocal ones by both tests. Percentages of invasive tumor were greater than 30% in all cases. A custom-designed PCR-based Illumina NGS assay including amplicons spanning the *HER2* locus and adjacent genes on chromosome 17 (as well as commonly mutated genes) were used to assess *HER2* copy number. Log₂-transformed signal levels averaged across the gene were normalized to a pool of non-amplified controls to derive a NGS-HER2 amplification score. The concordant samples were used to establish a cutoff for NGS-HER2 interpretation using the receiver operating characteristic method. This cutoff was then applied to equivocal or discordant cases.

Results: NGS amplification score for the 7 HER2 IHC+/FISH+ was 2.64 (1.25 to 4.35) and 0.22 (-0.85 to 1.25) for the 25 HER2 IHC-/FISH- with a cutoff of 1.0 achieving a sensitivity 100 % and a specificity 92.8%. After applying this cutoff to 13 equivocal specimens, all cases had negative NGS amplification scores. For FISH/IHC discordant cases, 18 out of total 21 were also negative for *HER2* amplification by NGS, while *PIK3CA*, *PTEN* and *TP53* mutation status was variable in those cases. Considering these discordant cases, NGS-HER2 score showed a higher concordance with HER2 FISH (Figure 1).



Conclusions: HER2 amplification by NGS demonstrates high concordance with both IHC and FISH methods. Nearly all FISH/IHC discordant or equivalent cases were reclassified as negative by NGS. Given the ability of this panel to also assess *BRCA1/BRCA2* and targetable mutations, NGS can be a single cost-effective method to assess simultaneously other clinically important genetic changes in breast cancer.

1970 Distribution of PD-L1 Gene Amplification Across 127,299 Solid Tumors and Hematologic Malignancies: Implications for Immune Checkpoint Inhibitor Therapies

Jeffrey S Ross¹, David Fabrizio², Garrett M Frampton², Lee Albacker¹, Ryan Hartmaier², Ethan Sokol², Alexa B Schrock³, Jon Chung², James Suh⁴, Shakti Ramkissoon⁵, Siraj Ali⁶, Vincent A Miller², Philip M Stephens², Julia A Elvin, Eric Severson⁷, Sugganth Danie², Laurie Gay. ¹Foundation Medicine, Cambridge, MA, ²Foundation Medicine, ³Foundation Medicine, Cambridge, MA, ⁴Foundation Medicine, Inc., Morrisville, NC, ⁵Foundation Medicine, Morrisville, NC, ⁶Cambridge, MA, ⁷Foundation Medicine, Inc., Morrisville, NC

Disclosures:

Jeffrey Ross: *Employee*, Foundation Medicine
David Fabrizio: *Employee*, Foundation Medicine
Ryan Hartmaier: *Employee*, Foundation Medicine
Ethan Sokol: *Employee*, Foundation Medicine
Alexa Schrock: *Employee*, Foundation Medicine
Jon Chung: *Employee*, Foundation Medicine
James Suh: *Employee*, Foundation Medicine
Shakti Ramkissoon: *Employee*, Foundation Medicine
Siraj Ali: *Employee*, Foundation Medicine
Philip Stephens: *Employee*, Foundation Medicine
Eric Severson: *Employee*, Foundation Medicine
Laurie Gay: *Employee*, Foundation Medicine

Background: The programmed death receptor ligand, PD-L1,

is encoded by the *PD-L1* gene (*CD274/B7H1*) has emerged as a major target of the immune checkpoint inhibitor (ICPI) class of immunotherapeutic drugs. Not currently a widely-recognized biomarker of therapy response, amplification of *PD-L1* has recently been linked to enhanced benefit of tumors to ICPI treatment.

Design: FFPE sections of 127,299 cases of clinically advanced malignancies encompassing more than 450 individual disease ontologies were sequenced using hybridization-captured, adaptor ligation-based comprehensive genomic profiling assay to a mean coverage depth of >500X for up to 315 cancer-related genes plus 37 introns from 28 genes frequently rearranged in cancer. *CD274 (PD-L1)* genomic alterations (GA) including gene amplification, short variant (SV) alterations and gene rearrangements were recorded for all tumor types. *PD-L1* amplification was determined using process matched controls (positive when ≥ 6 copies). PD-L1 protein expression was measured by immunohistochemistry (IHC) in a subset cases using the Dako 22C3 anti-PD-L1 antibody.

Results: 800 (0.63%) of 127,299 tumors featured *PD-L1* gene alterations: 782 (98%) were amplifications, 16 (2%) were short variant mutations and 2 (<0.1%) were gene rearrangements. Of the 10 common tumor types included in the Table, breast (205) and lung (198) carcinomas provided the greatest number of *PD-L1* amplified cases. When viewed as a percent of total cases with *PD-L1* amplification, head and neck squamous carcinomas (HNSCC) had the highest frequency at 2.5% followed by breast (1.4%), lung (0.7%) and bladder (0.6%) carcinomas. All other common tumor types had less than 0.5% frequencies of *PD-L1* amplification. There was a strong correlation between *PD-L1* amplification and expression of PD-L1 detected by IHC in NSCLC with 89% of *PD-L1* amplified NSCLC cases showing >50% IHC staining and 11% showing positive but <50% staining. Examples of major clinical responses to immune checkpoint inhibitor therapies for tumors featuring *PD-L1* amplification will be presented.

Tumor Type	Cases	Cases with PD-L1 Amplification	Percent
Breast Carcinoma	14,191	205	1.4%
Lung Carcinoma	26,155	189	0.7%
HNSCC	1,695	42	2.5%
Colorectal Carcinoma	12,952	18	0.1%
Glioblastoma	3,817	13	0.3%
Pancreatic Ductal Carcinoma	3,825	1	<0.1%
Ovarian Carcinoma	3,289	25	0.1%
Prostatic Carcinoma	3,041	7	0.2%
Melanoma	1,305	2	0.2%
Bladder Urothelial Carcinoma	1,699	11	0.6%

Conclusions: Amplification of *PD-L1* is an extremely rare event that occurs across many types of human cancers. *PD-L1* amplification is highly correlated with high membrane protein expression of PD-L1 measured by IHC and has been linked to significant durable response to ICPI therapies. Further evaluation of *PD-L1* amplification as a potential tumor type agnostic biomarker for immunotherapy selection appears warranted.

1971 Assessing Microsatellite Instability and Tumor Burden by Tumor-Normal Paired Whole Exome Sequencing

Wei Song¹, Juan S. Martinez². ¹Weill Cornell Medical College, ²Max Planck Tandem Group in Computational Biology, Universidad de los Andes, Bogotá, Colombia

Background: This year, FDA has approved two immune-checkpoint inhibitors for treating cancer patients with MSI-H or mismatch repair deficiency (dMMR). Molecular diagnosis of MSI is currently achieved by examining PCR products from a few (typically 5-7) informative microsatellite markers. However, there are a total of 19,05,236 microsatellites computationally identified across the human genome, and a comprehensive interrogation of MSI with a breadth and quantitative precision, such as assessing the data from Whole Exome Sequencing (WES), is still lacking. On the other hand, high tumor mutational burden (TMB) is an emerging biomarker of sensitivity to immune checkpoint inhibitor and has been shown to be more significantly associated with response to PD-1 and PD-L1 blockade immunotherapy than PD-1 or PD-L1 expression.

Design: 532 tumor-normal paired patient samples were sequenced in our institute. The WES BAM files were analyzed and each paired result was subjected to assessment of TMB and analysis by MSISensor (a software designed to analyze microsatellite in large data sets, including WES and whole genome sequencing), with the false-discovery rate set to 0.01. All statistical analyses were carried out using R.

Results: 1). On average, 5921 microsatellite sites were detected across 532 WES tumor-normal cases. 2). All experimentally proven MSI-high cases show a dramatic increase in MSI score and high

TMB (averages of 11.14 and 662 respectively), while all MSI-low cases exhibit much lower values for both of these variables (averages of 0.19 and 11 respectively). 3). Only 1.5% of the total WES cases are MSI-H according to MSISensor score, the latter having a significantly higher tumor burden (p -value<0.01) than those predicted or experimentally verified as MSI-L. 4). As expected, there is but a small correlation between number of microsatellite sites detected and MSISensor score (ρ =0.128, p -value<0.01), suggesting that the scoring process is not biased by the amount of microsatellite sites detected per sample.

Conclusions: MSI status assessment through WES data yields a 100% concordance with PCR-based test. The results also suggest the existence of a relationship between tumor burden and MSI status, with MSI-H cases having significantly higher tumor burden. Therefore, a comprehensive sequencing of patient's cancer cells not only could provide potential markers for target therapy, but also genomic status which can be used for other types of cancer treatment, including checkpoint inhibitor treatment.

1972 Xist Loss in Breast Cancer is Associated with Triple-Negative Hormone Receptor Status

Alexander Subtelny¹, Anna Biernacka², Vikram Deshpande¹, Elena Brachte¹. ¹Massachusetts General Hospital, Boston, MA, ²University of Chicago

Background: Dysregulation of epigenetic processes is a key driver event in many cancers. An important epigenetic event in the normal physiology of genetically female (XX) mammalian cells is X inactivation, which is mediated by a *cis*-acting, long non-coding RNA, *Xist*. This process results in an inactive X chromosome (Xi) that manifests microscopically as a Barr body. Breast cancer cells often show loss of the Barr body, due to either deletion or reactivation of the Xi. Using gene-expression data from The Cancer Genome Atlas (TCGA), we investigated whether female breast cancers downregulate *Xist* and whether this results in reactivation of the Xi.

Design: Transcriptome-wide gene-expression profiling data (generated by RNA-seq) was obtained from the TCGA. Breast cancers were separated into groups based on hormone receptor-expression status, and each group (ER+/PR+/HER-2-, ER+/PR+/HER-2+, or ER-/PR-/HER-2-) was divided further into two subsets: tumors with low *Xist* expression (designated *Xist*-low), and the remaining tumors (*Xist*-high). Of note, prior in situ hybridization (ISH) data had shown a higher proportion of triple-negative (ER-/PR-/HER-2-) tumors to be among tumors with low (43%) versus high *Xist* expression (28%). Relative expression levels for autosomal and X-chromosomal genes were then compared between *Xist*-low and -high tumors. Similar analyses were performed for select other tumor types.

Results: Triple-negative breast cancers expressed *Xist* at lower levels than ER+/PR+/HER-2- (2.83-fold, $P < 10^{-6}$) and ER+/PR+/HER-2+ tumors (2.67-fold, $P = 0.0003$). We also found that 6 of 10 pancreatic adenocarcinomas (PDAC) in female patients showed loss of *Xist* by ISH. Low *Xist* expression was not associated with significant upregulation of X-chromosomal genes in breast cancers. However, *Xist*-low PDACs exhibited modestly but significantly higher relative expression of X-chromosomal genes (1.07-fold, $P < 10^{-3}$). The three groups of *Xist*-low breast cancers often showed upregulation of several autosomal cancer-associated genes, such as *WNT5A* (up to 3.07-fold), *IL6ST* (an IL-6 receptor subunit; up to 5.32-fold), and *EGFR* (up to 4.44-fold).

Conclusions: Triple-negative breast cancers express *Xist* at lower levels than ER+/PR+/HER-2- and ER+/PR+/HER-2+ breast cancers. Low *Xist* levels are associated with increased relative expression of X-chromosomal genes only in PDAC, possibly due to derepression of the Xi. *Xist*-low breast cancers show increased expression of cancer-associated genes, such as *WNT5A*, *IL6ST* and *EGFR*.

1973 Low Tumor Burden and High Lymphocytic Infiltrate in On-treatment Biopsies is Significantly Associated with Response to Pembrolizumab in Patients with Rare Tumors

Coya Tapia¹, Mingxuan Xu², Fengying Ouyang³, Anas Alshawa², Joud Hajjar⁴, Lilibeth Castillo², Gopal Singh², Hung Le², Ravi Murthy², Aung Naing². ¹UT MD Anderson Cancer Center, Houston, TX, ²UT MD Anderson Cancer Center, ³UT MD Anderson Cancer Center, Houston, TX, ⁴Baylor College of Medicine / Texas Children's Hospital

Background: Treatment-induced morphological alterations are a well-known phenomenon and can be observed in on-treatment biopsies. The meaning of these alterations regarding prognosis and/or therapy response is unknown. The purpose of this study was to determine if morphological parameters such as e.g. tumor burden and lymphocytic infiltrate in tumors treated with pembrolizumab can be used as predictors for therapy response to immune checkpoint inhibitors.

Design: We investigated 77 baseline and 59 on-treatment (C1D15-21) tumors from 67 patients, enrolled in a phase II clinical trial receiving pembrolizumab for their rare tumors. Tumor burden (TB) and

lymphocytic infiltrate (LI) of biopsies were estimated on an H&E slide. Low TB was defined as $\leq 10\%$ tumor and LI was categorized into low and high. If more than one biopsy was available the average TB was calculated, and for the LI the highest value was used for analysis. The morphological data were correlated with clinical response, available from 54 (810.6%) patients. Response was defined as stable disease, partial or complete response.

Results: Low TB was observed in 29 (25%) of all tumors, in 17 baseline (27%) and in 12 on-treatment (24%) tumors. Forty-three percent (10/23) patients with low TB in their on-treatment tumor showed response compared to 5% (1/21) of non-responders, resulting in a significant association with response ($p=0.003$). High LI was observed in 52 tumors, 56% baseline and 44% on-treatment tumors. In 65% (11/17) patients with high LI in their on-treatment tumor showed response compared to 30% (6/20) of non-responders, resulting in a significant association with response ($p=0.035$).

Conclusions: Low TB and high LI in rare tumors treated with pembrolizumab were predictive for therapy response. Further studies are warranted to validate the role of TB and LI assessment on H&E stain and the cut-offs used as predictive parameters for immune checkpoint inhibitors.

1974 Genomic Integrative Pathology: A Large Scale Tumour Next Generation Sequencing Initiative

Basile Tessier-Cloutier¹, Jasleen Grewal², Martin Jones³, Erin Pleasance², Ellia Z Zhong⁴, Karen Mungall², Tae Hoon Lee⁵, Ellen Ca⁶, Brandon Sheffield⁷, Cheng-Han Lee⁸, Lien Hoang⁹, Brian Skinnider¹⁰, Tyler Smith¹¹, David Schaeffer⁸, Anna F Lee¹², Tony Ng¹³, Diana Ionescu¹, Torsten Nielsen¹⁴, Chris Dunham¹⁵, Steven Jones³, Janessa Laskin¹, Marco Marra³, Stephen Yip⁶. ¹British Columbia Cancer Agency, Vancouver, BC, ²Michael Smith Genome Sciences Center, ³Michael Smith Genome Sciences Center, ⁴University of British Columbia, Richmond, BC, ⁵University of British Columbia, ⁶University of British Columbia, Vancouver, BC, ⁷Vancouver, BC, ⁸British Columbia Cancer Agency, Vancouver, BC, ⁹Vancouver General Hospital, Vancouver, BC, ¹⁰Vancouver General Hospital, Vancouver, BC, ¹¹Vancouver General Hospital, ¹²Children's and Women's Health Centre of British Columbia, Vancouver, BC, ¹³University of British Columbia, Vancouver, BC, ¹⁴Univ. of British Columbia, Vancouver, BC, ¹⁵Children's & Women's Health Centre of British Columbia

Background: The discovery of genomic drivers of cancer behavior has revolutionized clinical oncology, pathology, and molecular diagnostics. Increasingly, companion molecular tests are used to prognosticate survival and to predict response to traditional and particularly molecular targeted therapeutics. The Personalized OncoGenomics (POG) program at the BC Cancer Agency has profiled whole genomes and transcriptomes on over 700 cancer patients with metastatic disease to deliver therapeutically relevant results in a clinically relevant time frame.

Design: Population scale combination of whole genome and transcriptome sequencing (WGS/WTS) and bespoke bioinformatic analytic pipelines of metastatic malignancies. Detailed review of each genomic report, clinical history, morphologic features and immunohistochemical profile was performed to determine how it could be integrated to inform diagnosis, prognosis and management. The cases were classified as "confirming", "augmenting", "re-aligning" the diagnosis or "failed" to add to the pathology report.

Results: The cohort of 494 cases included tumours from all sites, the most common being breast, gastrointestinal and bone and soft tissue. Overall, 381 (77%) confirmed, 51 (10%) augmented, 20 (4%) re-aligned the diagnosis and 43 (9%) failed. Primary of unknown origin (67%), skin (28%), central nervous system (27%), and lung tumors (24%) were the most likely to be augmented or re-aligned by integrating genomic analyses. Within the subset of 8 re-aligned PUGOs, 3 cases were diagnosed as cholangiocarcinoma and 5 other different tumour types (hepatocellular carcinoma, sarcoma, salivary gland adenocarcinoma, lung adenocarcinoma, and renal cell carcinoma).

Conclusions: Pathology, in the guise of glass-based histomorphology and the use of immunohistochemical profiling, remains an integral part of this analysis. In fact, integration of "traditional" tissue-based pathology metrics empowers the bioinformatic analytic pipeline and in some cases, is indispensable in the data analysis. The integration of immunohistochemistry with gene expression and a catalogue of genomic aberrations provides a comprehensive, multidimensional view of the cancer tissue. This approach was particularly useful in tissue from cancer of unknown primaries.

1975 DNA Methylation Profiling of Early T1/T2 Node-Negative Oral Cavity Cancers Identifies Potential Markers of Nodal Recurrence

Emilija Todorovic¹, Rebecca Towle², Cheryl Tan³, Yazeed Alwelaie¹, Eitan Prisman³, Cathie Garnis², Tony Ng⁴. ¹Vancouver, BC, ²BC Cancer Agency, ³University of British Columbia, ⁴University of British Columbia, Vancouver, BC

Background: Oral squamous cell carcinoma (OSCC) often portends a poor prognosis, particularly in the setting of cervical nodal metastasis. However, a significant subset of clinically small and node-negative (cT1/T2 cN0) tumors show no recurrence despite tumor resection alone. Ideally, a biomarker would be available to identify such low-risk cases, sparing these patients unnecessary therapy, including elective neck dissection and radiotherapy. Although some histologic parameters (e.g. depth or pattern of invasion) and genetic changes (e.g. copy number alterations) have shown association with nodal recurrence risk, no parameter has emerged as a reliable predictor. We sought to investigate epigenetic changes (i.e. DNA methylation) as potential biomarkers of nodal recurrence.

Design: DNA methylation profiling using the Illumina 850K MethylationEPIC array was performed on formalin-fixed paraffin-embedded (FFPE) tissues from eight cases of locally resected early (cT1/T2 cN0) OSCC tumors, half of which showed subsequent cervical lymph node recurrence, and half showing no evidence of recurrence despite average follow-up of 5.6 years. Preprocessing, normalization and identification of differentially methylated regions (DMRs) and blocks (DMBs) was performed in the R statistical software environment using the Bioconductor package ChAMP.

Results: Recurrent and non-recurrent cases showed similar mean clinicopathologic parameters, including age (65 vs. 59 years), tumor size (20 vs. 19 mm), depth of invasion (5.8 vs. 5.5 mm), distance to margins and pattern of invasion, with no cases showing perineural or lymphovascular invasion. Seven DMRs and 98 DMBs were identified (corrected p -values < 0.05). Two DMRs showing the most significant hypermethylation in recurrent versus non-recurrent cases involved a CpG island in 6p22.1 upstream of GABBR1, and a CpG island in 8q24.3 upstream of ARHGAP39; both regions have been previously implicated in oral cavity cancers.

Conclusions: Despite the similarity in clinicopathologic parameters between these recurrent and non-recurrent OSCC cases, statistically significant DMRs and DMBs could be identified within this early discovery cohort using FFPE samples. This justifies further investigation by methylation profiling of a larger cohort of similar cases, with the ultimate goal of developing a methylation-based biomarker of nodal metastasis risk in OSCC to guide surgical and oncologic therapy.

1976 Aldolase A Triggers Oct4 Activation to Acquire Lung Cancer Stem Cell Phenotypes through Non-Enzymatic Functions

HsingFang Tsai¹, Yu-Chan Chang, Michael Hsiao². ¹Academia Sinica, Taipei, ²Academia Sinica

Background: Aldolase A (ALDOA) is involved in glycolysis process. The enzyme can exert its function to catalyze Fructose 1, 6-bisphosphate to glyceraldehyde 3-phosphate and dihydroxyacetone phosphate. In recent years, several reports focusing on exploring the non-enzymatic role of ALDOA to control proliferation and/or enhance metastasis ability in cancer. However, its roles in cancer stemness remain unclear.

Design: We established the ALDOA-based transcriptomics and proteomics database to explore its functional roles in lung cancer stemness. Through Genespring software to normalization, we have selected candidate targets for prediction potential upstream regulator and pathway by Ingenuity Pathway Analysis (IPA) that may be mediated the induction of lung cancer stemness.

Results: Our data showed that ALDOA overexpressing resulted in significant increase in lung cancer spheres. We found that high expression of ALDOA, Oct4 and related cancer stemness markers in collected sphere cells. Furthermore, we designed specific mutant form ALDOA to block the enzymatic activity and wild-type ALDOA expression still induced significant *in vitro* sphere formations and *in vivo* tumorigenicity. We also identified several molecules involving ALDOA-Oct4 binding. Knockdown of these molecules could significantly decrease stemness ability in lung cancer. In addition, the established ALDOA transcriptomics database in our study identified the candidate drug that significantly suppressed Oct4 activation-induced axis signaling and suppressed ALDOA induced *in vitro* and metastasis *in vivo*.

Conclusions: Our study reveals novel ALDOA functional roles in inducing cancer stemness through activating Oct4 transcriptomic responses. The findings may provide new therapeutic strategies to modulate lung cancer stemness ability to enhance chemotherapeutic responses in lung cancer patients.

1977 Metabolic Protein Phosphoglycerate Kinase 1 Is Overexpressed in Lung Cancer and Promotes Metastasis

Yu-Wen Tseng¹, Yu-Chan Chang¹, Michael Hsiao². ¹Academia Sinica, Taipei, ²Academia Sinica

Background: The dysregulated metabolism is an emerging hallmark of cancer. However, little is known about the metabolic requirements

during cancer progression.

Design: *In-silico* data mining and shRNA screenings were performed to identify key-metabolic genes associated with lung cancer metastasis. Functional overexpression and complementary knockdown were assayed to reveal the identified gene phenotypes in metastasis. Clinical correlations of the identified genes were evaluated to determine their prognostic values in lung cancer patients.

Results: By using the integrated transcriptomics data and the shRNA library against glycolytic enzymes, here we find that Phosphoglycerate Kinase 1 (PGK1) up-regulation highly correlates with migratory/invasive activity of lung cancer cells and poorer outcomes in clinical lung cancer patients. These findings were validated by Immunohistochemistry (IHC) staining for PGK1 antibody against clinical lung cancer tissues. Significantly, the knockdown of PGK1 inhibited but the enforced expression of exogenous PGK1 promoted the *in vitro* and *in vivo* migratory/invasive activity of lung cancer cell lines that highly or poorly expresses PGK1 protein, respectively. Through connectivity map database mining, we also identified candidate drug and their therapeutic effects in *in vivo* lung cancer models. Molecular imaging analyses of the animals with lung cancers showed that the compounds prevented distal metastasis and decreases *in-situ* lung nodule formation ability and prolonged animal survivals. Importantly, PGK1 can be served as an independent prognostic factor and positively correlated with recurrences, and poor survival rates in lung cancer patient cohorts.

Conclusions: Our results identified PGK1 metabolic gene that induced cancer invasion/metastasis and may provide a novel target for cancer prognosis and therapy.

1978 The NGS Solid Tumor Panel Gene Count "Arms Race": Why Bigger Isn't Always Better

Eric Vail¹, Jianbo Song², Jing Xu², Joseph S Frye³, Andy Pao², Angela Aguiluz², Wenjuan Zhang², Serhan Alkan⁴, David Berz⁵, David Engman⁶, Jean Lopategui⁷. ¹Cedar-Sinai Medical Center, Los Angeles, CA, ²Cedars-Sinai Medical Center, ³Cedars Sinai Medical Center, Los Angeles, CA, ⁴Cedars Sinai Med Ctr, ⁵Beverly Hills Cancer Center, ⁶Los Angeles, CA, ⁷West Hollywood, CA

Background: Next generation sequencing (NGS) of cancer gene panels has begun to supplant single gene testing in cancer molecular diagnostics. Clinical panels have evolved to include differing numbers of genes, with inverse relationships between coverage and turnaround time. The largest panels contain hundreds of genes, many having no associated FDA approved therapies, medically useful clinical trials or prognostic implications. Some feel that the information provided by these large panels is only incrementally greater than that provided by a panel containing a few dozen genes, and can also be misleading to both clinicians and patients. At the same time, many believe that "bigger is better" with the incremental additional information worth the higher cost and turnaround. We compared the results of testing of a large panel from a reference lab to the 161 gene panel utilized by the National Cancer Institute (NCI).

Design: NGS reports from a large reference lab panel covering over 300 genes were retrospectively analyzed to determine whether the reported genomic alterations would have been detected by the NCI panel. Differences in each patient's eligibility for FDA approved therapy (for intended use and off label) and selection for clinical trials were assessed. For statistical analysis, all reference lab reported drugs and clinical trials were considered valid and all discrepancies were assessed for clinical relevance.

Results: 483 large panel reports were analyzed, which reported a cumulative 2078 genomic alterations. Eighty-three (17%) patients had mutations associated with FDA approved therapy, 272 (56%) qualified for off label therapy and 397 (82%) were eligible for clinical trials. The NCI panel covered 1360 (65.4%) of the alterations detected by the large panel. Importantly, all (100%) of the patients identified as eligible for FDA and off label therapies were identified by the NCI panel. 389 (97.9%) of the patients identified as eligible for clinical trials were also identified by the NCI panel. The 8 remaining patients not covered by the NCI panel were all phase I studies with early investigational compounds.

Conclusions: While the large commercial panel detected more alterations than the NCI panel, the additional alterations had no impact on clinical management. All patients determined to qualify for an FDA or off label therapy would be identified by either panel. Only 2% (8/397) of patients eligible for a phase 1 clinical trial were only identified by the larger panel.

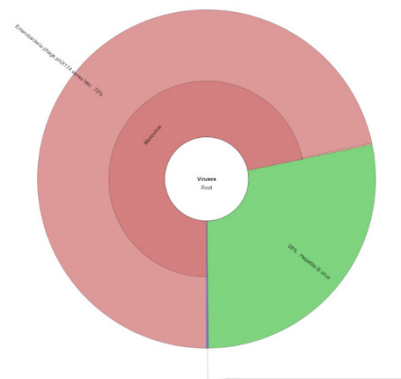
1979 Mining Large Panel Hybrid Capture-Based Clinical NGS Data for Novel Virus Pathogen-Tumor Associations Based on Mapping of Off-Target Reads to Viral Genomes

Chad M Vanderbilt¹, Jonathan Reiche², Ahmet Zehi³, Maria Arcila⁴, Snjezana Dogan⁵, Marc Ladany⁶, Sumit Middha². ¹Memorial Sloan Kettering Cancer Center, New York, NY, ²Memorial Sloan Kettering Cancer Center, ³MSKCC, ⁴New York, NY, ⁵Memorial Sloan-Kettering, New York, NY, ⁶Memorial Sloan-Kettering CC, New York, NY

Background: Viral pathogens, including human papillomavirus (HPV) and Epstein Barr virus (EBV), are known to be oncogenic. The number of viral pathogens is so numerous that, heretofore, it has been intractable to screen large numbers of diverse tumor types for viral associations. In hybrid capture (HC) enrichment for NGS analysis of tumors, the HC probes incidentally capture reads from outside the targeted regions, including tumor-associated viral DNA reads that can be mapped to a full spectrum of virus-specific genomes. We currently employ MSK-IMPACT™, a clinically validated HC based NGS assay for detection of somatic alterations in the genomes of tumor samples. Here we show that HC Off-Target Mapping to virus genomes (OTM-virus) from MSK-IMPACT can be used to detect the presence of pathogens and results correlate well with orthogonal clinical assays.

Design: From our database of previously sequenced paired FFPE tumor and blood normal DNA samples, we identified tumor types with known virus associations. These samples were tested with a clinically validated testing platform for in situ hybridization (ISH) of the viral nucleic acid (i.e. HPV and EBV) and correlated with OTM-virus results. We then interrogated a subset of our database for additional viruses and correlated these findings with tumor types.

Results: We identified 54 archived head and neck carcinomas with MSK-IMPACT and ISH results. Concordance in virus identification between OTM-virus and ISH was 46/49 (94%) for HPV and 4/5 (80%) EBV, respectively. False negatives (n=3) could be attributed to low tumor purity and a low number of off-target DNA reads. The case (n=1) that was positive by OTM-virus but negative by ISH is likely due to detection limitations of the historical DNA-ISH assay in a p16 positive case by immunohistochemistry. Figure 1 shows a view of the hierarchical visualization tool employed (Kronos) showing hepatitis B sequence in a hepatocellular carcinoma.



Conclusions: This study is proof of principle that we can confidently screen the remainder of our large cohort of sequenced tumor samples for viral DNA using this novel approach for the purpose of the discovery of additional virus-tumor associations. We have several candidate, previously undescribed, tumor-virus associations that require further verification. This approach can be expanded for the identification of other pathogen types that would be challenging to explore with a narrow approach.

1980 Germline DNA Repair Single Nucleotide Polymorphism (SNP) in Urothelial Carcinoma (UC)

Aram Vosoughi¹, Panagiotis J Vlachostergios², Tuo Zhang³, Samaneh Motanagh⁴, Brian Robinson⁵, Olivier Elemento⁶, Bishoy M Faltas⁷, Mark Rubin⁸, Juan Miguel Mosquera⁸. ¹Weill Cornell Medicine / Englander Institute for Precision Medicine New York, NY, ²Weill Cornell Medicine New York, NY, ³Elmhurst, NY, ⁴Weill Cornell Medicine, New York, NY, ⁵Weill Cornell Medicine, New York, NY, ⁶New York, NY, ⁷Weill Cornell Medicine, ⁸Weill Cornell Medical College, New York, NY

Background: Association of DNA damaging agents such as cigarette smoke and aniline dye with the risk of bladder cancer is well known. DNA damaging chemotherapy agents like platinum-based chemotherapy improve the overall survival of Muscle Invasive Urothelial Carcinoma (MIUC) and repair of DNA damage is key in the development of chemo/radiation therapy resistance. We aimed to identify germline DNA Repair Genes (DRG) SNPs, that may be enriched and potentially associated with outcome in UC.

Design: 53 patients (median age 64, 42 males) with MIUC were

enrolled in our IRB-approved Precision Medicine Program and received platinum-based chemotherapy. Patients' Family History (FH) of cancer in first-degree relatives and Smoking History (SH) were recorded. 43 patients had primary bladder UC and 10 had UC of upper tract. Germline DNA extracted from blood lymphocytes or buccal swabs was used as the control for Whole Exome Sequencing (WES) and examined for DRG SNPs. As a reference for SNP frequencies, the Exome Aggregation Consortium (ExAC) database was used. Correlation of SNPs of DRG with FH of cancer and SH was calculated by Pearson correlation coefficient. Overall Survival (OS) was compared with Log-rank test.

Results: Twelve different SNPs were identified among 6 DNA repair pathways (DRP). The frequency of DRG SNPs in our cohort (15/53, 28%) is significantly higher than ExAC database (0.44%, Chi-square $p < 0.01$). There was no significant difference in OS between patients with and without DRG SNPs ($p = 0.117$). Germline DRG SNPs show slight correlation with FH of cancer and SH among patients with MIUC (R: 0.3, $p = 0.036$, R:0.2 $p < 0.05$). Nucleotide excision repair (NER) pathway showed the highest SNPs frequency (5/53, 9.4%). Frequency of micropapillary UC, small cell carcinoma and sarcomatoid features is higher in cases with SNPs of DRG (6/15, 40%).

Conclusions: Germline SNPs of DRG are more common in UC, compared to general population and could play a role as biomarkers of risk to develop UC and response to treatment. SNPs of DRG are more common in morphologic UC variants with clinical significance. The study of larger cohorts of MIUC with similar stage could help clarify the prognostic significance of germline DRG SNPs.

1981 Notch Inhibition Suppresses Acute Promyelocytic Leukemia Cell Line Proliferation Through Cell Cycle Regulation

Eric X Wei, Shreveport, LA

Background: Notch signaling pathway plays an essential function in hematopoietic tumorigenesis. In contrast to its well-defined role in T-cell lymphoblastic leukemia, the impact of Notch pathway in acute myeloid leukemia (AML), particularly acute promyelocytic leukemia (APL) remains controversial. Some group found it is suppressed in AML, while others reported Notch signaling is activated in AML. Here we used AML cell lines HL-60 and KG-1 to study the effects of Notch signaling on leukemia cell proliferation, cell cycle regulation, and mitochondria functions.

Design: APL cell line HL-60 and AML cell line KG-1 from ATCC were cultured in IMDM medium. They were treated with Notch inhibitor DAPT and LY-411575, and Notch activator Jagged-1 for 48 hours. After harvesting the cells, RNA were extracted for RT-PCR of Notch downstream target gene HES1 expression. Cells were concentrated using cytology cell block techniques for immunohistochemistry of antigens CD117, myeloperoxidase, and BCL-2 expression in leukemia cells. Cells were fixed for electron microscopic examination. Cells are collected for mitochondrial function using JC-1 mitochondrial membrane potential assay and MitoTracker Red CMXRos assay by flow cytometry.

Results: 48 hours treatment of KG-1 cells did not have definitive effects on HES1 gene expression. Incubation using Notch inhibitor LY-411575 and DAPT significantly decreased HES1 gene expression levels in HL-60 cells, particularly LY-411575. Notch activator Jagged-1 markedly increased HES1 mRNA levels. By electron microscopy, LY-411575 and DAPT inhibited cell proliferation and growth with significantly increased heterochromatin and apoptotic cells in HL-60 cells, particularly LY-411575. In contrast, Jagged-1 increased the percentages of euchromatin and proliferating cells. There was no significant difference in mitochondrial numbers and morphology between treatment groups. JC-1 and MitoTracker Red CMXRos assays showed similar findings in mitochondrial functional assays. There were also no significant differences of antigen expressions of CD117, myeloperoxidase, and BCL-2 between different treatment groups.

Conclusions: Notch inhibitors suppress acute promyelocytic leukemia cell proliferation through cell cycle regulation by increased heterochromatin and apoptosis, and downregulation of its downstream target gene HES1. Notch inhibitors do not seem have significant effects on mitochondrial functions in APL. More studies are underway to elucidate Notch effects in APL cells.

1982 Oncogenic Activating Cyclin D1 Mutations are Enriched in Endometrioid Endometrial Adenocarcinomas

Jia Xu¹, Douglas I Lin¹. ¹Beth Israel Deaconess Medical Center, Boston, MA

Background: Cyclin D1 (*CCND1*) is a core cell cycle regulator and is frequently overexpressed in human cancers, often via amplification, translocation or post-transcription regulation. Accumulating evidence suggests that mutations of the *CCND1* gene that result in nuclear retention and constitutive activation of CDK4/6 kinases are oncogenic

drivers in cancer. However, the spectrum of *CCND1* mutations across human cancers has not been systematically investigated.

Design: Here, we retrospectively mined whole-exome sequencing data from 94 published studies representing 24,212 cases from diverse cancer types via online data mining tools to determine the frequency and spectrum of *CCND1* mutations in human cancers and their associated clinicopathological characteristics.

Results: Overall, in contrast to gene amplification, which occurred at a frequency of 5.4% (1,151 of 21,047 cases), *CCND1* mutations were of very low frequency (0.46%, 112 of 24,212 cases) across all cancers, but were predominantly enriched in uterine endometrioid-type adenocarcinoma (6.5%, 30 of 458 cases) in both primary tumors and in advanced, metastatic endometrial cancer samples. *CCND1* mutations in endometrial endometrioid adenocarcinoma occurred most commonly in the C-terminus of cyclin D1 as putative driver mutations, in a region thought to result in oncogenic activation of cyclin D1 via inhibition of Thr-286 phosphorylation and nuclear export, thereby resulting in nuclear retention and protein overexpression.

Conclusions: Our findings implicate oncogenic mutations of *CCND1* in the pathogenesis of a subset of human cancers, provide a key resource to guide future investigations and suggest that select endometrial cancer patients may potentially benefit from targeting cyclin D1-CDK4/6 complexes with CDK4/6-specific inhibitors, such as palbociclib.

1983 High Dose Platinum Induces Cell Death via Mitotic Catastrophe in High Grade Serous Carcinoma Cell Lines but Generates Rare Aneuploid Subpopulation of Tumor Cells

Tony Yu Wing Yeung¹, Oliver W Fung², Mikhail Bashkurov³, Robert Rottapel⁴, Andras Kapus⁵. ¹St. Michael's Hospital, Toronto, ON, ²McGill University, Markham, ON, ³Lunenfeld Research Institute, ⁴UHN, Toronto, ON, ⁵St. Michael's Hospital

Background: Platinum chemotherapy is part of the first-line treatment for high grade serous carcinomas (HGSC) of tubal-ovarian origin. DNA damage induced by platinum is thought to result in apoptosis through p53-mediated signaling. But in the background of mutant p53 in HGSC, it is less clear how DNA damage signaling results in cell death and whether alteration in the cell death pathway may promote platinum resistance. In this project, we demonstrate that high dose platinum induces mitotic catastrophe in HGSC cell lines, leading to cell death but that avoidance of mitotic cell death could be mediated through durable maintenance of the G2-M checkpoint or by survival in an aneuploid state after mitotic slippage events.

Design: We used a multiplex high-content fluorescence microscopy platform and a quantitative image-cytometry analytical approach to assess the kinetics of the DNA damage response, cell-cycle checkpoint activity and cell death after *in-vitro* carboplatin treatment on several HGSC cell lines (OVCAR3, TOV3133G). In addition, time-lapse microscopy was performed to assess mitotic events after carboplatin treatment.

Results: Carboplatin treatment induced cell cycle arrest at the G2 phase initially but at later time points permitted aberrant mitotic progression, leading to mitotic catastrophe and subsequent cell death. These aberrant mitotic events were shown by phospho-Histone-H3 staining and by time-lapse microscopy. The progression into mitosis was also accompanied by a paradoxical weakening of the CHEK signaling axis. Aberrant mitotic progression could be circumvented due to durable G2-M checkpoint, which was exhibited by an *in-vitro* derived carboplatin-resistant cell line. More interestingly, mitotic cell death was a frequent but not unanimous outcome as rare tumor cells managed to survive through mitotic slippage events and then entered an aneuploid state.

Conclusions: This study illustrates that cell death caused by platinum drugs may depend on mitotic catastrophe and that the G2-M checkpoint is a critical regulator of mitotic cell death. Resistance mechanisms circumventing mitotic cell death could be due to durable G2-M checkpoint or survival post mitotic slippage events. The rare aneuploid tumor cells may harbor the potential for regrowth and be resistant to further platinum challenges. We are currently phenotyping these platinum-induced aneuploid tumor cells further and assessing their potential for regrowth.

1984 NGS Panels Provide Supplementary Prognostic Information for Metastatic Lung Cancer

Wanying Zhang¹, Susan Hsiao², Carlos Pagan², Andrew Turk², Mahesh Mansukhan³, Anjali Saqi³, Helen Fernandes³, Anthony Sirec⁴. ¹New York Presbyterian Columbia University Medical Center, White Plains, NY, ²New York Presbyterian Columbia University Medical Center, ³Columbia University Medical Center, ⁴New York, NY, ⁵Columbia University Medical Center, New York, NY

Background: The updated NCCN Clinical Practice and the CAP/IASLC/ molecular testing guidelines emphasize the importance of

timely assessment of relevant genomic alterations in patients with non-small cell lung cancer (NSCLC). We assessed the impact of a 47gene NGS panel to further elucidate the diagnostic and prognostic utility of the assay.

Design: This is a retrospective analysis of 635 surgical and cytology samples from histologically confirmed primary or metastatic NSCLC, sequenced between January 2015 and August 2017. DNA was extracted from tissue that was macrodissected to enrich for lesional cells. Variants were detected using a targeted NGS panel on the Illumina MiSeq platform. TTF1 expression was determined by immunohistochemistry (IHC). FISH or IHC was used to detect *ALK* gene rearrangements.

Results: 94% of the cases presented as adenocarcinoma and 16.3% of the tumors sequenced were from metastatic lesions. The landscape of individual *EGFR* variants detected in 23.8% of the cases was similar to previously reported. Overall, 19.9% of the *EGFR* positive tumors harbored compound *EGFR* alterations with the T790M resistance mutation being the additional variant in about 10% cases. Almost 90% of the *EGFR* mutant cases were concomitantly tested for *ALK* rearrangements, as per guidelines and interestingly 3/132 cases, that were metastatic, showed a concurrent *EGFR* variant and *ALK* rearrangement. *PIK3CA* variants were present in 4.1% of the tumors. More than 50% of the *PIK3CA* mutated cases harbored concurrent alterations in *KRAS* and these tumors were from metastatic lesions. Furthermore, mutations in the helical domain of *PIK3CA* (E545K and E542K) were present in 78% of the co-mutated cases, indicating likely increased aggressiveness. In our cohort, 33.3% of the cases were found to harbor *KRAS* alterations with a preponderance of transversion(66%) over transition(34%) mutations ($P<0.05$). IHC revealed that 99% *EGFR* mutant tumors analyzed were positive for TTF1 expression compared to 78% of NSCLC with *KRAS* alterations ($P<0.05$).

Conclusions: In accordance with the NCCN guidelines, the molecular information offers substantial therapeutic options for patients with mutated NSCLC. Overabundance of *KRAS* transversion mutations and concurrent mutations in *KRAS* and the helical domain of *PIK3CA* in metastatic NSCLC may have prognostic relevance. TTF1 expression correlates with the *EGFR* mutation status in NSCLC.